Deterministic icehouse and greenhouse climates throughout Earth history

Tyler Kukla[1], Kimberly V. Lau[2], Daniel E. Ibarra[3,4], Jeremy K. C. Rugenstein[1]

[1]Department of Geosciences, Colorado State University, Fort Collins, CO
[2]Department of Geosciences and Earth and Environmental Systems Institute, The Pennsylvania State University, University Park, PA
[3]Department of Earth, Environmental and Planetary Sciences, Brown University, Providence, RI
[4]Institute at Brown for Environment and Society, Brown University, Providence, RI, USA

This is a non-peer reivewed preprint submitted to EarthArXiv

Corresponding author: Tyler Kukla, tykukla@colostate.edu

Deterministic icehouse and greenhouse climates throughout Earth history

Tyler Kukla[1], Kimberly V. Lau[2], Daniel E. Ibarra[3,4], Jeremy K. C. Rugenstein[1]

[1]Department of Geosciences, Colorado State University, Fort Collins, CO
[2]Department of Geosciences and Earth and Environmental Systems Institute, The Pennsylvania State University, University Park, PA
[3]Department of Earth, Environmental and Planetary Sciences, Brown University, Providence, RI
[4]Institute at Brown for Environment and Society, Brown University, Providence, RI, USA

Corresponding author: Tyler Kukla, `tykukla@colostate.edu`

Abstract

Some theories posit that icehouse (with polar ice sheets) and greenhouse (ice-free) states throughout Earth history are not deterministic, but bistable—both states may occur for the same level of radiative forcing. If correct, then the climate state that persists for millions of years can depend on which state already existed, giving the system a 'memory' effect. However, on these timescales the negative silicate weathering feedback in the long-term carbon cycle stabilizes global climate—a feedback which is missing from models that simulate a bistable system. Here, we test whether bistability persists on million-year timescales with a model that couples climate, weathering, and the long-term carbon cycle. We show that transitions between bistable states put the long-term carbon cycle out of balance and silicate weathering restores this balance, collapsing bistability. On million-year timescales any memory effect disappears, and the state of global climate is largely deterministic.

1 Introduction

Over the course of Earth history, our planet has cycled between icehouse and greenhouse climate states (with and without large polar ice sheets) that often span millions of years. The mechanisms behind these long-term cycles remain a first-order question in the Earth sciences. One set of theories posits that these cycles are driven by external forcings to the Earth system that modify the long-term carbon cycle, such as changes in long-term solid Earth degassing of CO_2 (Berner, 1991, 2004, 2006; Herbert et al., 2022; Lee et al., 2013; McKenzie et al., 2016; McKenzie & Jiang, 2019; Van Der Meer et al., 2014) or internal processes such as changes in the efficiency of weathering reactions that sequester CO_2 (Caves et al., 2016; Caves Rugenstein et al., 2019; Krissansen-Totton & Catling, 2017; Kump & Arthur, 1997; Macdonald et al., 2019; Swanson-Hysell & Macdonald, 2017). Under these theories, the state of global climate is deterministic—it can be unambiguously determined if the external forcings and internal processes are known.

Alternatively, work based on energy balance climate models and ice sheet models calls into question the role of external forcings in icehouse-greenhouse transitions. These studies often find that the Earth system displays bistability, whereby an icehouse or a greenhouse climate state can exist at the same level of external forcing, usually represented by the partial pressure of atmospheric CO_2 (pCO_2) (Fig. 1A) (Budyko, 1969; Dortmans et al., 2019; Ferreira et al., 2011; Kypke & Langford, 2020; Pohl et al., 2014; Pollard & DeConto, 2005; Rose & Marshall, 2009; Sellers, 1969; Stap et al., 2017). A bistable system is not deterministic because, within the 'bistability window' (Fig. 1A), its state cannot be unambiguously determined from the external forcings and internal processes. When more than one stable state is possible, the realized state depends on the memory, or past state, of the system. For example, an icehouse and greenhouse are both possible at T_2 in Fig. 1A, but an icehouse is realized because the system was previously in an icehouse state at T_1. In a bistable climate, a small, short-lived forcing can irreversibly tip the system from one state to the other—the memory of the system allows the new state to persist indefinitely after the forcing has ceased.

Icehouse-greenhouse bistability emerges most strongly due to the positive ice-albedo feedback whereby warming melts high-albedo ice, decreasing the amount of reflected sunlight, causing more warming and melting more ice (or, conversely, cooling expands ice coverage, causing more cooling) (Budyko, 1969; Ferreira et al., 2011; Rose et al., 2017; Sellers, 1969). Although most common in simpler energy balance models (Abbot et al., 2011; Budyko, 1969; Rose & Marshall, 2009; Sellers, 1969), icehouse-greenhouse bistability has also been identified in fully coupled Earth System Models (Ferreira et al., 2011; Pohl et al., 2014). The exact mechanisms for bistability vary across the model hierarchy, but positive non-linear radiative feedbacks, such as the ice-albedo feedback, are critical in supporting multiple equilibria in all cases (DeConto & Pollard, 2003; Murante et al., 2020; Pollard & DeConto, 2005; Schneider et al., 2019).

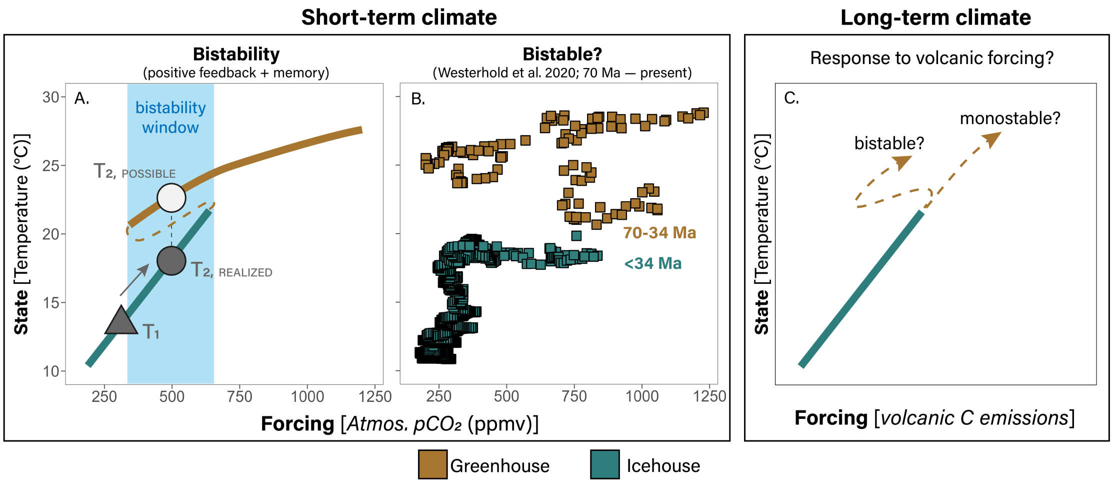

Figure 1. Bistability scenarios and Cenozoic data. (**A**) Classical icehouse-greenhouse bistability. T_1 represents the prior state of the system (the state it "remembers"). Filled T_2 circle shows the realized state at some later time, and open T_2 circle is a mathatically possible equilibrium. (**B**) Paleoclimate data over the last 70 million years show multiple stable temperature solutions for some values of atmospheric CO_2 (Westerhold et al., 2020). (**C**) Long-term (million-year) bistability landscape where the forcing is CO_2 emissions, not the atmospheric CO_2 concentration.

Recent work suggests that transient nudges between bistable states can explain major icehouse-greenhouse transitions in Earth history (Dortmans et al., 2019; Kypke & Langford, 2020; Pohl et al., 2014; Pollard & DeConto, 2005; Stap et al., 2017). In the Cenozoic ($\sim 66-0$ Ma) and Ordovician ($\sim 485-443$ Ma), for example, modeling work has linked the establishment and persistence of ice sheets to the climate system's memory after crossing some critical threshold (Dortmans et al., 2019; Kypke & Langford, 2020; Pohl et al., 2014; Pollard & DeConto, 2005; Stap et al., 2017, 2022). These model results imply that the memory of the climate system is indefinite. Once the state of the system changes, there are no internal processes (*i.e.*, negative feedbacks) that operate to restore the system to its original state. Consequently, long-lasting climate transitions can occur with minimal external forcing. Indeed, external drivers of icehouse-greenhouse transitions are not always obvious from paleoclimate data and they remain intensely debated (Elsworth et al., 2017; Jagoutz et al., 2016; Lefebvre et al., 2013; McKenzie et al., 2016; Park et al., 2020; Pohl et al., 2014; Rugenstein et al., 2021).

The debate surrounding whether global climate is deterministic has focused on why bistability is more robust in simple models and less so in complex models, and the implications for paleoclimate—such as whether short-lived forcing can cause long-lived climate change—are largely seen as hinging on these results (Dortmans et al., 2019; Ferreira et al., 2011; Kypke & Langford, 2020; Pohl et al., 2014; Rose & Marshall, 2009; Rose et al., 2017; Stap et al., 2017; Valdes, 2011; Zeebe, 2011). However, the models at the center of this debate—both simple and complex—do not explicitly represent known negative feedbacks in the long-term carbon cycle that play out on million-year timescales (Ferreira et al., 2011; Kypke & Langford, 2020; Pohl et al., 2014; Rose & Marshall, 2009; Stap et al., 2017). The primary known negative feedback is the silicate weathering feedback, which is considered a pre-requisite for planetary habitability because it tends to restore climate after a perturbation, preventing runaway climate states (Archer, 2005; Sagan & Mullen, 1972; Walker et al., 1981). Such a negative feedback should act against the positive ice-albedo feedback by limiting the memory of the climate system and therefore its potential to exhibit bistability. In this way, whether the climate system is deterministic depends on the timescale—climate could be bistable on short timescales but deterministic on longer timescales when long-term carbon cycle feedbacks, primarily negative feedbacks, must be considered.

Here, we test whether icehouse-greenhouse transitions are deterministic over geologic timescales ($> 10^6$ yr), assuming the climate system is bistable but also subject to known long-term negative feedbacks that operate in the geologic carbon cycle. To do so, we use a newly developed model (Kukla et al., 2022b) that couples an energy balance climate model capable of simulating bistable states (Flannery, 1984; Frierson et al., 2006; Hwang & Frierson, 2010; Rose et al., 2014; Roe et al., 2015; Siler et al., 2018) with a model for rock weathering (Caves et al., 2016; Ibarra et al., 2016; Maher, 2011; Maher & Chamberlain, 2014; Winnick & Maher, 2018) and a one-box model of the long-term exogenic carbon cycle (Berner, 2006; Caves et al., 2016; Caves Rugenstein et al., 2019; Shields & Mills, 2017). Previous work has investigated exoplanet habitability with related frameworks, coupling a weathering model or carbonate chemistry model with a lower-order energy balance climate model (Abbot et al., 2012; Graham & Pierrehumbert, 2020; Graham, 2021), though these studies did not explicitly simulate the long term evolution of the carbon cycle as implemented here.

In this work, we show that there is only one global temperature solution that balances the long-term carbon cycle for a wide range of climate forcings and continental configurations. Short-term bistability causes more than one possible global temperature for a given pCO_2 level, but the alternative temperature state puts the carbon cycle out of balance. Thus, so long as a negative feedback acts to maintain a balanced carbon cycle, the memory of the climate system is ultimately limited by the response time of this negative feedback in collapsing the alternative temperature state. We further define a bistability framework that accounts for the distinct forcing mechanisms of long-term climate and discuss key considerations when using paleoclimate data to test icehouse-greenhouse bistability. Our results emphasize that even if the climate system can exhibit bistability, the long-term climate state is generally deterministic as the geologic carbon cycle collapses short-term bistability to a single, stable state.

2 Long-term climate and bistability

The long-term habitability of our planet depends on global temperatures being warm enough that water does not freeze and cool enough that it does not boil (or, more restrictively, cool enough for macroscopic life to survive) (Kasting, 1993; Sagan & Mullen, 1972). On timescales short enough that the solar luminosity flux is constant (but long enough for exogenic carbon fluxes to impact pCO_2), varying volcanic emissions are the largest source of greenhouse gases and, thus, climatic change. If these emissions are not balanced by the removal of greenhouse gases, the climate system can "runaway" and become too hot (similar to Venus today) or too cold (similar to Mars). Modeling the long-term carbon cycle shows that even small imbalances ($<$ 10%) between emissions and sequestration can cause a runaway climate within a few million years (Berner & Caldeira, 1998; D'Antonio et al., 2020). Thus, it has long been understood that some negative feedback must allow carbon sequestration via burial in some form to respond to emissions to maintain habitability.

This negative feedback is widely thought to depend on the weathering of silicate rocks (Berner & Caldeira, 1998; Maher & Chamberlain, 2014; Walker et al., 1981). As pCO_2 increases, a more intense hydrologic cycle and warmer temperatures cause more silicate weathering which transfers atmospheric pCO_2 to alkalinity and, ultimately, sequesters it as carbonate minerals (Urey, 1952; Velbel, 1993; Walker et al., 1981). This negative silicate weathering feedback represents the primary distinction between short-term and long-term climate. Atmospheric pCO_2 forces climate but, on million-year timescales, climate influences atmospheric pCO_2 via silicate weathering. In this case, pCO_2 is not the external forcing of the climate system because it is implicated in internal feedbacks which affect the balance between inputs and outputs of CO_2. Instead, solid Earth carbon degassing (or carbon sequestration, recognizing that degassing and sequestration must balance on long timescales) is the appropriate external forcing (McKenzie & Jiang, 2019) (Fig. 1C). In turn, factors such as tectonics and rock weatherability may also act as a forcing on climate by causing weathering fluxes to change (Bluth & Kump, 1994; Caves Rugenstein et al., 2019; Kump & Arthur, 1997; Raymo & Ruddiman, 1992; Penman et al., 2020). As we will discuss later, a natural consequence of this distinction is that climate bistability on long timescales must be evaluated relative to volcanism (the external forcing) rather than atmospheric pCO_2 (*e.g.* Veizer et al. (2000)).

The last $\sim$ 66 million years, the Cenozoic Era, presents a useful case study for considering the likelihood of long-term climate bistability (Kypke & Langford, 2020; Stap et al., 2017). Cenozoic proxy data for temperature and pCO_2 are abundant, global climate existed in both a greenhouse (66−34 Ma) and icehouse (34 Ma-present) state, and previous work has argued that these states could be bistable (Dortmans et al., 2019; Kypke & Langford, 2020; Pollard & DeConto, 2005; Stap et al., 2017). If the long-term climate system is bistable, the most recent greenhouse-icehouse transition $\sim$ 34 million years ago may be the product of pCO_2 falling below a critical threshold or tipping point (DeConto & Pollard, 2003; Pollard & DeConto, 2005; Pearson et al., 2009; Goldner et al., 2014), with the memory of the climate system allowing the new icehouse state to persist, influencing global climate for millions of years (Pollard & DeConto, 2005; Kypke & Langford, 2020; Stap et al., 2017). Indeed, absent other long-term forcings, if pCO_2 returned to its prior greenhouse levels after the icehouse transition then climate memory is required to explain the icehouse's persistence. Some atmospheric pCO_2 compilations show that the same pCO_2 level can yield an icehouse or a greenhouse climate (Fig. 1B) (Westerhold et al., 2020). Others, however, show a smaller or absent bistable window (Foster & Rohling, 2013; Rae et al., 2021), and it is not clear whether temperature-CO_2 bistability can accurately diagnose long-term climate bistability.

3 Methods

Our simulations are run with the newly developed Carbon-H_2O Coupled HydrOlOgical model with Terrestrial Runoff And INsolation, or CH2O-CHOO TRAIN. This model combines a zonal mean energy balance climate model with components for the weathering of minerals and the fluxes of the long-term carbon cycle. Each sub-model is described in more detail in Kukla et al. (2022a) and below, along with information on how the models are coupled. Code and documentation for the CH2O-CHOO TRAIN can be found in Kukla et al. (2022b).

3.1 The energy balance model

We use an energy balance model that simulates zonal mean climate by balancing net atmospheric heating ($Q_{\rm net}$; $W\ m^{-2}$) with the divergence of northward moist static energy transport (Flannery, 1984; Frierson et al., 2006; Hwang & Frierson, 2010; Rose et al., 2014; Roe et al., 2015; Siler et al., 2018). The model is built on equation 1, relating $Q_{\rm net}$ to the latitudinal gradient of column-integrated moist static energy (h; $J\ kg^{-1}$) and a constant coefficient for diffusive energy transport (D; m^2s^{-1})

$$Q_{net}(x) = -\frac{p_s}{ga^2}D\frac{d}{dx}\left[\left(1-x^2\right)\frac{dh}{dx}\right] \quad (1)$$

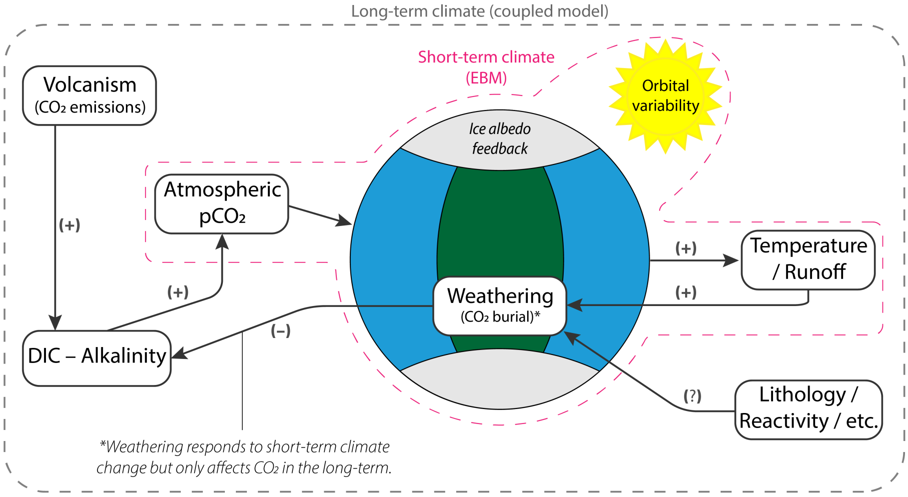

Figure 2. Coupled model schematic. Atmospheric pCO_2, the initial climate state, and the ice albedo feedback determine the equilibrium climate state in the energy balance model (pink dashed outline, short-term climate system). On longer timescales, the climate state influences weathering, which draws down atmospheric pCO_2 (black dashed outline, long-term climate system). Volcanism (i.e. solid Earth degassing) is the primary external forcing for pCO_2 in the model. Plus and minus signs refer to the direction in which one term affects the next.

where p_s is air pressure at the surface (Pa), g is acceleration due to gravity ($m\ s^{-2}$), a is Earth's radius (m), x is the sine of latitude and $(1-x^2)$ accounts for the planet's spherical geometry. Moist static energy, h, is defined as the sum of latent and sensible heating, $h = c_pT + L_vq(T)$, where c_p is the specific heat of air ($J\ kg^{-1}$), T is the near-surface temperature ($°C$), L_v is the latent heat of vaporization ($J\ kg^{-1}$), and q is specific humidity ($g\ kg^{-1}$), a function of temperature via the Clausius-Clapeyron relationship. We prescribe Q_{net} based on the balance of non-reflected incoming radiation and energy lost to space where

$$Q_{\text{net}}(x) = Q_0(x)(1 - \alpha(x)) - (A + BT(x)). \tag{2}$$

The first term on the right of equation 2 is the source term, defined as the balance of incoming and outgoing shortwave radiation where the incoming shortwave (Q_0) is multiplied by one minus albedo (α) at latitude x. The second term is the sink term where outgoing longwave radiation linearly depends on temperature T via a coefficient (B) that captures the effect of the water vapor feedback and an intercept (A) that depends on pCO_2 (Budyko, 1969; Koll & Cronin, 2018; Siler et al., 2018; North et al., 1981).

Based on the moist static energy output, the model solves for precipitation and evaporation, employing the modifications for upgradient Hadley cell transport, following Siler et al. (2018). These precipitation and evaporation fluxes hold for zonal mean conditions over the ocean, where there is an infinite supply of water to evaporate, but they are not readily applicable to terrestrial conditions where evaporation is often limited by water availability. As a result, this zonal mean scaling by itself can produce unreasonable results over land on long timescales, such as evaporation outpacing water supply (Siler et al., 2018). To address this shortcoming, we estimate terrestrial evapotranspiration (ET; $kg\ m^2\ s^{-1}$) and runoff based on the balance of precipitation (P; $kg\ m^2\ s^{-1}$) and potential evapotranspiration (E_0 taken as the oceanic evaporation; $kg\ m^2\ s^{-1}$) using the Budyko hydrologic balance framework (Budyko, 1974; Fu, 1981; L. Zhang et al., 2004). Here, runoff is a fraction (k_{run}) of P with the fraction determined by

$$k_{run} = 1 - \frac{ET}{P} = \frac{E_0}{P} - \left[1 + \left(\frac{E_0}{P}\right)^{\omega}\right]^{1/\omega} - 1. \tag{3}$$

Equation 3 is a version of the Budyko equation where ω is a free parameter that determines the efficiency with which precipitation is partitioned into evapotranspiration versus runoff. We assign the global average ω of 2.6 for all simulations (Fu, 1981; L. Zhang et al., 2004; Greve et al., 2015).

3.2 Weathering Model

Though the weathering model is described in detail elsewhere (Maher & Chamberlain, 2014; Winnick & Maher, 2018), we briefly outline the primary equations and parameters here. To encapsulate the role of climate in modifying weathering fluxes, we use the reactive transport framework of Maher and Chamberlain (2014). The silicate weathering flux ($F_{\mathrm{w,sil}}$; $mol\ kyr^{-1}$) is calculated via:

$$F_{\mathrm{w,sil}} = Q \times C[sil] \tag{4}$$

where $C[sil]$ is the concentration of silicate derived solutes ($mol\ 1000L^{-1}$) and Q is discharge ($m^3\ kyr^{-1}$) calculated from the product of runoff and land area. In this reactive transport framework, temperature affects $C[sil]$ via an Arrhenius relationship; runoff, in turn, modifies $C[sil]$ via dilution. Reaction rates are parameterized with a Damköhler weathering coefficent which reflects the rate of fresh supply of minerals and their lithology. Though not implemented in this paper, varying this coefficient permits testing how spatially variable lithologies and erosion rates may alter the time-transient evolution of the Earth system following a perturbation. The theoretical maximum $C[sil]$ ($C[sil, eq]$) is modified by the weathering zone pCO_2, according to the relationships presented in Winnick and Maher (2018). Weathering zone CO_2 is calculated following the system of equations presented in Volk (1987).

3.3 Carbon Cycle Model

The geological carbon cycle model calculates the mass balance of the dissolved inorganic carbonate (DIC) and alkalinity reservoir pools as a function of the primary fluxes of carbon and alkalinity. Inputs of carbon include volcanism, carbonate weathering, and petrogenic organic carbon weathering and outputs of carbon include carbonate burial and organic carbon burial. The alkalinity mass balance comprises inputs of carbonate weathering and silicate weathering and the primary output is carbonate burial. We speciate the carbonate system using the parameters of (Zeebe & Wolf-Gladrow, 2001) and assume equilibrium between atmospheric CO_2 and oceanic CO_2. Carbonate burial is parameterized as a first-order relationship with the calcite saturation index, Ω, in the ocean (Caves Rugenstein et al., 2019; Stolper et al., 2016) and organic carbon burial is parameterized as a first-order relationship with the carbonate burial flux (Caves Rugenstein et al., 2019; Ridgwell, 2003).

3.4 Coupling the energy balance model with the weathering and carbon cycle components

We run long-term steady state and time-transient simulations with different model couplings. In our steady state simulations, we only couple the energy balance climate model with the weathering model (Fig. 2). To accomplish this, we first define a control simulation that provides a baseline for the latitudinal distribution of temperature and continental runoff. These temperature and runoff fields are fed into the weathering model at each latitudinal box and the global weathering flux is determined by integrating the latitudinal profile. This global flux is then scaled via a constant coefficient to match a prescribed initial volcanic degassing rate, satisfying the steady state condition whereby weathering (carbon sequestration) balances volcanism (carbon emissions). This coefficient acts to modify the strength of the weathering feedback, and we hold it constant for all steady state and time-transient simulations so the output is directly comparable. The weathering model then uses deviations in temperature and runoff from the baseline climate state to simulate changes in weathering fluxes, providing an internally consistent weathering response to changing climatic parameters. In steady state simulations, weathering fluxes are calculated but have no effect on climate—volcanism in these runs is implicitly assumed to change 1:1 with weathering and no perturbations to the system are imposed.

The key difference between our steady state and time-transient simulations is the inclusion of time-dependence in the long-term carbon cycle. With this time-dependence, atmospheric pCO_2 responds to imbalances between volcanism and weathering, increasing when there is excess volcanism and decreasing when there is excess weathering. The time-transient simulations also require defining a baseline climate and weathering coefficient, after which point the model is run forward in time using a fourth order Runge-Kutta algorithm with the *pracma* package in R (Borchers, 2021).

3.5 Bistability in the energy balance model

Bistability emerges in the energy balance model based on the numerical calculation. The set of energy balance model equations can be solved as a boundary value problem using the *bvpcol* function from the *bvpSolve* package in R (Mazzia et al., 2014). To solve the set of equations, we prescribe an initial guess of temperature at each pole and set the moist static energy flux at both poles to zero (zero-flux boundary condition). The initial temperature guess captures the effect of memory in the model. If we initialize the model with polar temperatures that would cause glaciation, the model will settle into an icehouse climate if a stable icehouse is possible. For the same set of conditions, the model will produce a greenhouse climate if initial polar temperatures are above the glaciation threshold and a stable greenhouse is possible.

Our simulations can be run with bistability turned on or off. When bistability is turned off we use the same initial temperature guesses for all simulations (one pole above the glaciation threshold, and one pole below). When bistability is turned on, the initial temperature guess is prescribed based on the previous timestep in the time-transient simulations, and prescribed by the user in the steady state model. In the time-transient runs, we initialize the model in an icehouse if the previous timestep produced an icehouse climate and, alternatively, in a greenhouse if the previous timestep produced a greenhouse climate. If the model tries to transition from one state to the other, we verify that this transition also occurs in a series of test scenarios where the pCO_2 and initial temperature conditions are "nudged" by $< 1ppmv$ and $< 1°C$, respectively. If all test scenarios produce the new climate state, the state transition is deemed robust and is accepted. If even one scenario produces the previous climate state, the previous state persists. This robustness test for icehouse-greenhouse transitions only occurs when bistability is turned on, and it effectively prescribes a high level of "inertia" in the climate system. This inertia makes it harder for the model to change from one climate state to the other and, thus, maximizes the size of the bistability window (the blue box in Fig. 1A).

3.6 Model experiments

We conduct four sets of simulations that address (1) the distinction between short and long-term climate bistability; (2) the silicate weathering response to climate and continentality; (3) the memory of the climate system; and (4) a general estimate of the long-term climate bistability window.

Experiments 1-3 use a control climatology baseline, where the internal parameters and feedback strengths follow previous calibrations based on modern climate (Hwang & Frierson, 2010; Roe et al., 2015; Siler et al., 2018) and climate sensitivity is tuned to $\sim 4-6°C$ of warming per doubling of pCO_2 (Knutti et al., 2017). We use a single, control climatology here to focus on how the system responds to different forcings and continental configurations holding all else constant. In experiment 4, we explore a wide range of internal parameters, radiative feedback strengths, and climate sensitivities in an effort to constrain the limits of long-term climate bistability.

3.6.1 Bistability in the short and long-term climate system

We first analyze the response of the climate system in our model to a reversible, $1.5x$ forcing in three simulations (Fig. 3A). In each case, the energy balance model retains memory of the previous climate state—it is initialized in an icehouse if the previous timestep produced an icehouse, or a greenhouse if the previous timestep produced a greenhouse. The first run is a "short-term climate" simulation (see Fig. 2) where atmospheric pCO_2 is the external forcing, and the long-term carbon cycle is not considered. The model is run in multiple forcing steps in steady state mode, grounded in an initial baseline climate. In these forcing steps, pCO_2 steadily ramps up to $1.5x$ the initial value, then ramps down symmetrically back to the initial value (Fig. 3A). In the second run, the initial baseline climate state is identical, but long-term climate constraints (where weathering acts on pCO_2) are included, and the forcing on the system is a $1.5x$ increase in volcanism (not pCO_2). Atmospheric pCO_2 evolves based on the balance of volcanism and weathering. Unlike in the first simulation, this long-term simulation requires running the model in time-transient mode to allow a new steady state to be reached for each new level of volcanic forcing. To accomplish this, we run the model for 750 kyr at each forcing level (each point in Fig. 3C) permitting the model to reach a new steady-state, and we calculate the steady state climatology (plotted) based on the average of the last 175 kyr (effectively "spinning up" the model at each new forcing step). This approach is functionally equivalent to (but computationally less expensive than) changing volcanism so slowly that the long-term carbon cycle is always in balance. We only plot the equilibrated results for the long-term simulation, but output from the full, time-transient model evolution can be found in Supplemental Fig. S1.

The third simulation repeats the second, but accounts for the effect of orbital forcing on incoming solar insolation. Orbital forcing introduces noise to the climate system that can cause icehouse-greenhouse thresholds to be crossed earlier, limiting the region of bistability. Pollard and DeConto (2005), for example, found that orbital forcing diminished the memory of distinct stable states in an ice sheet model that exhibits hysteresis (a memory effect). We compute the last 8.25 million years (11 volcanic forcing steps for 750 kyr each) of annual mean insolation forcing using the global astronomical parameters of Laskar et al. (2004) to calculate the latitudinal insolation distribution following Berger (1978) and Berger et al. (2010) as implemented in the *palinsol* package in R (Crucifix, 2016). Insolation forcing is then updated within the exogenic carbon cycle numerical solver based on the solver's timestep. We note that our model does not capture seasonality, and thus will not resolve the seasonal climate variations induced by orbital forcing that often drive the long-term mean climate and carbon cycling (*e.g.* De Vleeschouwer et al. (2020); Gosling and Holden (2011); Tigchelaar and Timmermann (2016)). Thus, orbital cycles in our model likely underestimate the true effect of orbital forcing on climate and its long-term variability.

3.6.2 Weathering response to climate and geography

To test the relationship between silicate weathering and global runoff in our coupled model, we simulate climate and weathering for a range of atmospheric pCO_2 levels using five idealized geographic configurations (Fig. 4). These geographic configurations include a vertical "Cat-eye" configuration of land, a "Midland" configuration with midlatitude continents, "Northland" with a polar continent (inspired by Laguë et al. (2021)), "Subtropicland" with subtropical continents, and "Tropicland" with a single belt of land across the tropics. Note that, while these geographies are displayed in two-dimensions for simplicity (Fig. 4), there is no zonal asymmetry as the model computes zonal mean climate. All simulations are conducted in steady-state mode (no time dependence). Thus, while we solve for the flux of carbon burial due to silicate weathering, we implicitly assume that emissions and removal fluxes of atmospheric CO_2 are balanced. To directly compare each configuration with the same set of boundary conditions, we define the silicate weathering feedback strength coefficient such that the weathering flux for the Cat-eye configuration at 280 ppmv pCO_2 is 8×10^{12} moles C/yr (Bachan & Kump, 2015), and we use the same coefficient for all simulations.

3.6.3 Climate memory

We run the fully coupled, time-transient model with the Cat-eye and Subtropicland geographies at a range of initial atmospheric pCO_2 levels to constrain the memory of the climate system at different weathering sensitivities. In each model run, an additional 3.3×10^{18} moles of carbon are emitted via volcanism (relative to background) over the span of 100 kyr. After 100 kyr, the external forcing returns to its initial, background level. We calculate the memory of the climate system based on how long a new climate state (*i.e.*, icehouse or greenhouse) is sustained after the 100 kyr forcing ends. For example, an icehouse that transitions to a greenhouse during a transient carbon cycle perturbation, but recovers to an icehouse after 250 kyr would have a climate memory of 250 kyr. In contrast, by this definition, the memory is zero if the initial climate state is restored before the forcing ends, and the memory is not defined if the forcing does not cause the climate state to change at all.

The key distinction between this climate memory calculation and a carbon cycle "recovery time" is the definition of the initial state (*e.g.* Archer (2005); Caves et al. (2016)). The climate memory is set by the time when the initial climate state (*i.e.*, icehouse or greenhouse) is recovered, whereas the recovery time often refers to the point when the initial global temperature is recovered, or when balance is restored between carbon emissions and burial. Thus, a greenhouse climate that is perturbed to a warmer greenhouse can have a well-defined recovery time, but no defined climate memory because the state of global climate did not change. In contrast, when the climate system is perturbed from an icehouse to a greenhouse (or vice versa) the climate memory and recovery time will be similar. Because the recovery time can impact climate memory, bistability is not required in the energy balance model for memory to be non-zero. Therefore, to constrain how bistability affects climate memory independent of the system recovery time, we repeat the above simulations with bistability turned off, making the energy balance model fully deterministic.

3.6.4 Estimating the long-term bistability window

In our final set of simulations, we explore how the long-term bistability window changes in a wide range of climate conditions. We run six sets of experiments, each calculating how the bistability window responds to a broad range of values for a given model parameter. The six parameters that we test are (1) climate sensitivity to pCO_2 (A in equation 2); (2) the strength of the water vapor feedback (B in equation 2); (3) the diffusivity coefficient (D in equation 1); (4) ice albedo (effectively the strength of the ice albedo feedback); (5) land albedo (indirectly affects the ice albedo feedback strength); and (6) the temperature threshold for ice to form. Tests 4-6 serve to modify the strength of the ice albedo feedback by either changing the difference between land/ocean and ice albedo, or allowing ice to form at higher or lower temperatures (though always below $0°C$).

For each of the six model parameters, we run the coupled model in steady state mode (energy balance model plus weathering model assuming weathering balances volcanism) for every 5 ppmv of pCO_2 across the entire short-term bistability window. Steady state mode is used because our goal is to constrain the bistability window on steady state timescales (> 1 million years). At each pCO_2 level, we test at least 10 different orbital configurations that approximate an eccentricity cycle, and we test two sets of temperature boundary conditions (one for icehouse and one for greenhouse) for a total of 20 simulations. The bistability window is bounded by the pCO_2 level where all 20 simulations return a greenhouse climate (the upper-bound) or all 20 simulations return an icehouse climate (the lower-bound).

However, this bistability window overestimates the true bistability window in the short and long-term climate because it is the sum of all orbital configurations. That is, the lower-limit occurs at the orbital configuration that produces the lowest-pCO_2 greenhouse and the upper-limit occurs at the orbital configuration that produces the highest-pCO_2 icehouse. The bistability window for any single orbital configuration (as in the short-term climate) is likely more limited. Long-term climate bistability is even more restricted because, at a given pCO_2, the stable climate state must persist for effectively *all* orbital configurations, not just a few.

Thus, to constrain the long-term bistability window, we develop an approach that accounts for orbital variability but is less strict than requiring a climate state to persist for all orbital configurations, providing a broader (more conservative) estimate of the long-term bistability window. In this approach, we calculate the fraction of orbital configurations where, if the model is initialized in an icehouse (greenhouse) the model will result in an icehouse (greenhouse). In other words, we calculate the fraction of orbital configurations that do not change the initial climate state. We refer to this fraction of simulations as the "stable fraction" and it is calculated for each climate state (icehouse or greenhouse) at every pCO_2 level. A stable fraction of one means that orbital forcing will not change the climate state for a given pCO_2. A stable fraction of 0.6 means that 40% of orbital configurations will cause the climate state to change at that pCO_2 level.

Using this stable fraction metric, we deem a climate state (icehouse or greenhouse at a given pCO_2) unstable in the long-term when (1) the stable fraction for that climate state is low *and* (2) the stable fraction for the alternative climate state is sufficiently higher. Any stable fraction less than 0.75—meaning that one quarter of orbital configurations would cause an icehouse-greenhouse transition—is deemed low enough to be unstable because the initial climate state is unlikely to persist for a full orbital cycle. In these cases, we then deem the climate state unstable only if the alternative state's stable fraction is at least 0.15 greater, making it more stable. When these two conditions are met for a given level of pCO_2—the initial climate state has a stable fraction of < 0.75 *and* the alternative state's stable fraction is at least 0.15 greater—then the initial climate state at this pCO_2 is considered unstable in the long-term and does not contribute to the bistability window.

In the above framework, the lower-bound of the long-term bistability window is the lowest pCO_2 level where a greenhouse is stable (stable fraction > 0.75 or stable fraction < 0.75 *and* no more than 0.15 below the icehouse value). The upper-bound of the bistability window is the highest pCO_2 where an icehouse is stable (stable fraction > 0.75

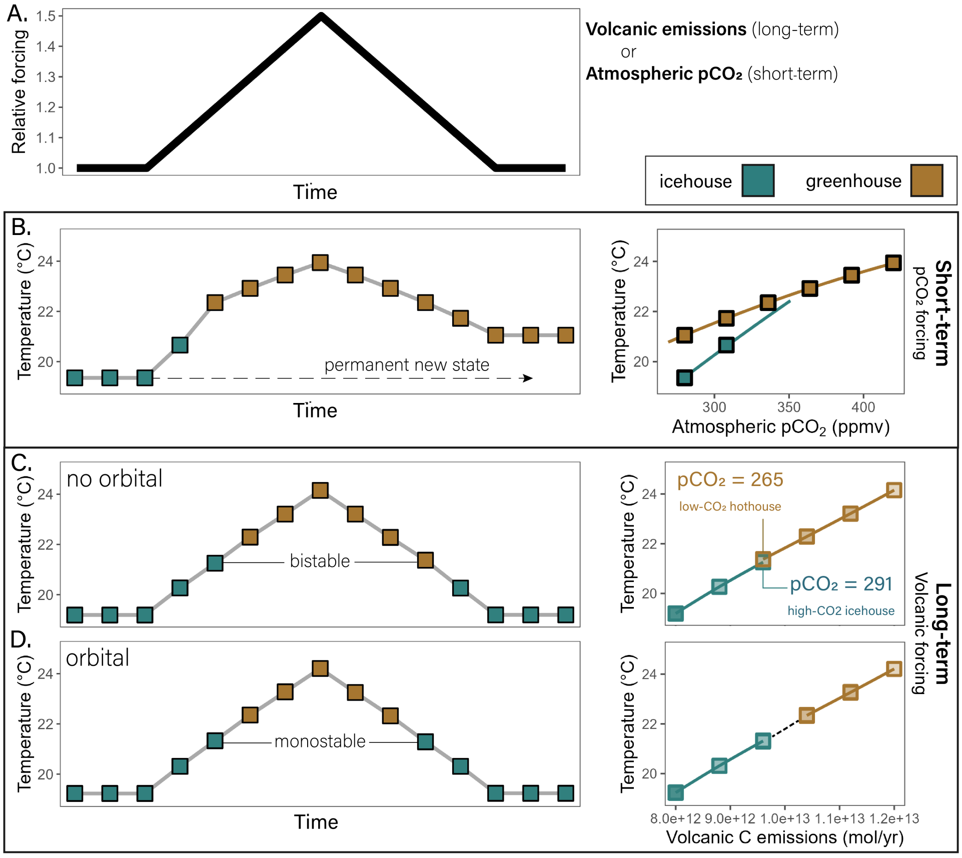

Figure 3. Long-term carbon cycle and orbital forcing collapse bistability. (**A**) Forcing normalized forcing over time. Refers to pCO_2 change for panel (B) and volcanic emissions for panels (C, D). (**B**) Climate response in the energy balance model (short-term system) only. Temperature does not return to its initial state even though the forcing does return to its initial state. (**C, D**) The equilibrated climate response to long-term carbon cycle-climate dynamics. Without orbital forcing, a small bistability window emerges where two climate states (icehouse and greenhouse) exist for the same temperature (C). With orbital forcing, this bistability window disappears and the climate state is fully deterministic (D).

or stable fraction < 0.75 *and* no more than 0.15 below the greenhouse value). Long-term, bistability is the range of volcanic degassing (assumed equal to weathering) that this window covers. The bistability window is zero (a fully deterministic climate) when there is no volcanic degassing level that could support both a long-term stable icehouse and greenhouse climate.

4 Results

4.1 Short and long-term climate bistability

Consistent with previous work (Dortmans et al., 2019; Hyde et al., 1999; Kypke & Langford, 2020; Pohl et al., 2014; Pollard & DeConto, 2005; Stap et al., 2017, 2022) our model exhibits hysteresis, or a memory effect, when the constraints of the long-term carbon cycle are ignored. In Figure 3, a 1.5x increase in pCO_2 causes a shift to a greenhouse climate that is sustained even when pCO_2 decreases back to its initial value (Fig.

3B). The climate system "remembers" its new greenhouse state even after the forcing that caused the transition to a greenhouse state ends. This is a bistable result—the right panel of Fig. 3B shows that more than one state (icehouse vs greenhouse) can exist for the same forcing (atmospheric pCO_2). This simulation does not have any negative feedbacks capable of restoring the original state; consequently, the new greenhouse state will persist indefinitely.

Inclusion of the long-term carbon cycle, however, shrinks the range of bistability. Here, volcanic emissions (not pCO_2) increase by $1.5x$ and act as the forcing on the system. Note that "Time" on the x-axis effectively refers to "forcing steps" (see Methods). As volcanic emissions and global temperatures increase, climate transitions to a greenhouse state (Fig. 3C, "no orbital"). This new state persists until volcanism and temperature decline sufficiently to restore the icehouse state. While the final state is identical to the initial state, there is still a small bistability window in the "no orbital" simulation. At a global temperature of ~ 22 degrees, the equilibrated, long-term climate system can exist in either a low-CO_2 greenhouse ($CO_2 = 265$) or a higher-CO_2 icehouse ($CO_2 = 291$) (Fig. 3C, "no orbital" right panel). This bistability is possible because both states have the same global weathering flux that can balance volcanic emissions. Thus, a limited window of long-term climate bistability is possible in our model, but only when an icehouse and greenhouse climate have similar weathering fluxes which generally requires similar global temperatures.

Our results from the "orbital" simulation, however, show that even the diminutive, long-term bistability window is fragile. The variability in mean annual insolation due to orbital forcing erases the low-CO_2 greenhouse state, returning the system to the more stable higher CO_2 icehouse (Fig. 3D, the "orbital" panels). As in the "no orbital" simulation, there is a single stable temperature for any given forcing (volcanism). However, unlike "no orbital", the "orbital" simulation also produces a single climate state (icehouse or greenhouse) for each level of forcing. In other words, we find no long-term bistability in our "orbital" simulation. As mentioned in section 3.6.1, our "orbital" simulation likely under-represents the true climate noise induced by orbital forcing because it ignores precession and seasonal feedbacks that can amplify the long-term mean response. Orbital forcing primarily affects global temperature in our model, and the simulated temperature response to orbital variations is about $0.1°C$. This temperature response is likely substantially smaller than the global temperature changes associated with orbital cycles for most of the Cenozoic (Lisiecki & Raymo, 2005; Westerhold et al., 2020; Zachos et al., 2001). Nonetheless, orbital variability, along with the long-term carbon cycle feedbacks, fully collapses the bistability window that exists in the short-term simulation. Full, time-transient output for Figure 3C is plotted for reference in the supporting information.

4.2 Weathering response to climate change

The increase in silicate weathering with warming is a robust feature in our model that collapses short-term climate bistability. The strength of the silicate weathering feedback is determined by the magnitude of the weathering response to climate—if the feedback is strong, then weathering increases rapidly with warming (Caves et al., 2016; Isson et al., 2020; Penman et al., 2020). Thus, the factors that drive silicate weathering—primarily temperature and runoff in our model—dominantly determine the strength of the silicate weathering feedback.

We find that global terrestrial runoff increases with warming in each idealized geographic configuration except for the Subtropicland world (Fig. 4A). Here, runoff increases slightly with initial warming as ice sheets melt, but decreases with further warming in a greenhouse climate. The decrease in runoff with warming is a consequence of decreasing precipitation with warming in the subtropics, although whether runoff declines in the subtropics as pCO_2 rises in more complex general circulation climate models remains controversial (Byrne & O'Gorman, 2015; Burls & Fedorov, 2017). In all other configurations, runoff increases with warming. The kink-point in the Northland world simulation occurs at the icehouse-greenhouse transition—runoff increases faster with warming in an icehouse state because of the combined effect of warming plus ice sheet retreat exposing more land area for water runoff. In the greenhouse state, the ice-free land area does not change with climate and the runoff sensitivity to warming decreases. While the runoff response to warming is uncertain in complex Earth System Models, the CMIP5 ensemble predicts a global runoff increase of 2.9%/K with warming (X. Zhang et al., 2014), broadly consistent with our results for a range of continental geographies.

The temperature and runoff outputs of the energy balance model, when used to drive the weathering model, yield a positive change in silicate weathering with warming. This weathering response to warming is shown in Figure 4B, where the y-axis reflects the normalized weathering (burial) or volcanic (emissions) CO_2 flux as we assume steady state in these scenarios. The shape and relative slope of the weathering response to warming is broadly consistent with that of the runoff response. However, in the Subtropicland world, weathering increases slightly with warming despite a decrease in runoff; in short, rising temperatures increase concentrations of weathered material, driving an increase in the weathering flux despite a decrease in global discharge.

4.3 Climate memory

The memory of the climate system in our model is ultimately limited by the time required for the geologic carbon cycle to return to steady-state—the carbon cycle's recovery time. This recovery time depends in part on whether the energy balance model (short-term climate) is run with bistability turned on. The recovery time also increases when the silicate weathering feedback is weak (the increase in weathering flux with incremental warming is small). Figure 5 illustrates this point. The climate system "remembers" its previous state for longer in the Subtropicland world, where the weathering response to climate is weak (see Fig. 4B), compared to the Cat-eye geography where the weathering response is stronger (Fig. 5D).

Our results also show that a bistable climate, by itself, increases the memory of the system. When bistability is turned off (Fig. 5B and faded lines in Fig. 5D) the system takes less time to return to the original climate state. The bistable simulations take longer to return in part because we impose a high degree of "climate inertia" (see Section 3.5). However, this result is also due to the bistable climate system needing to overshoot the initial temperature to return to the initial state. Figure 5C outlines how, after the icehouse-greenhouse transition (arrow 1), a bistable climate is temporarily within a greenhouse state (arrow 2) which it follows to a pCO_2 level that is below the initial pCO_2, then warms along the icehouse arrow until the original state is restored (arrow 3). This overshoot (arrows 2 and 3) can be seen in the global temperature response in Figure 5B. Reaching this overshoot point—the pCO_2 threshold where a greenhouse tips to an icehouse—takes more time when the greenhouse-icehouse pCO_2 threshold occurs at a temperature similar to the starting temperature (*i.e.* at higher initial pCO_2 values). The starting temperature corresponds with a balanced carbon cycle, so approaching the starting temperature (even from a different climate state) slows the rate of CO_2 drawdown by acting to balance the fluxes of weathering and volcanism. This effect explains why the change in memory with pCO_2 is less linear (more exponential) with bistability turned on. The initial state takes much longer to recover when the new climate state yields a weathering flux that can nearly balance volcanism (Fig. 5B). We note that once the initial pCO_2 is sufficiently greater than the control pCO_2 the model is initialized in a greenhouse state so there is no change in climate state (thus, no memory) across the volcanic perturbation. This greenhouse threshold happens after the initial minus control pCO_2 value reaches 50 ppmv in Subtropicland word, but before 50 ppmv in the Cat-eye geography, which is why the purple triangles extend to higher ΔpCO_2 values in Figure 5D.

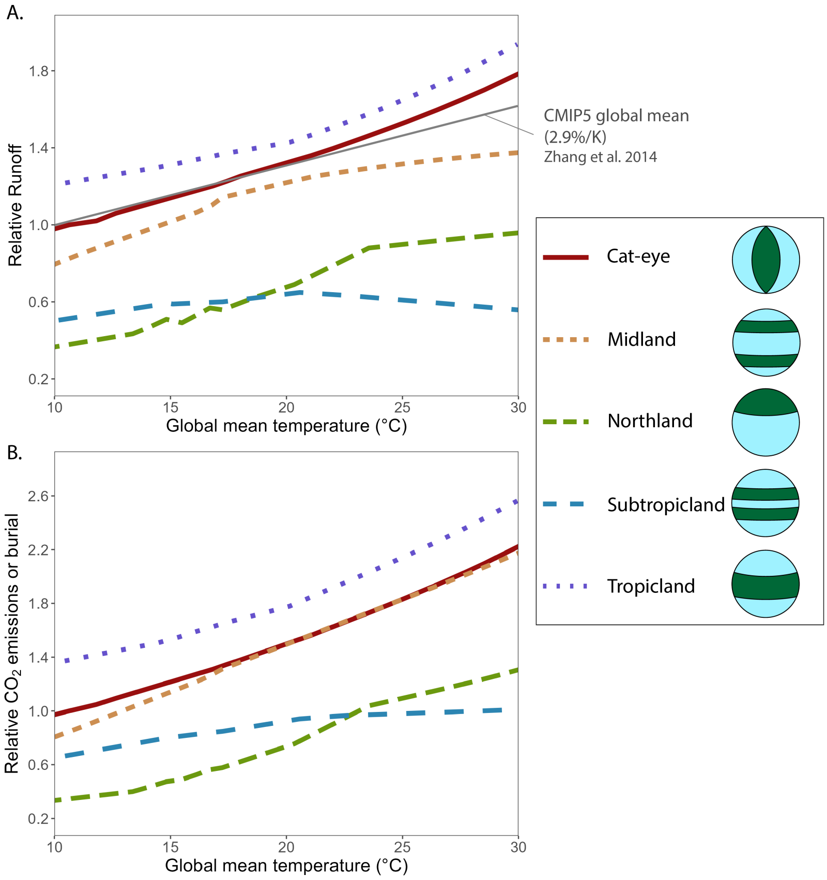

Figure 4. Climate impacts on weathering. (**A**) Global runoff increases with temperature in all geographies but the Subtropicland world. The slope and intercept differ depending on the geographic configuration, but many are similar to scaling in more complex models (gray line; X. Zhang et al. (2014)). (**B**) Due to the tight coupling between runoff and temperature, silicate weathering broadly tracks the runoff trends. Importantly, in all cases there is a single silicate weathering flux for a given global temperature, restricting the global temperature capable of balancing the long-term carbon cycle. All values are normalized to the Cat-eye world at $\sim 10^{\circ}$C.

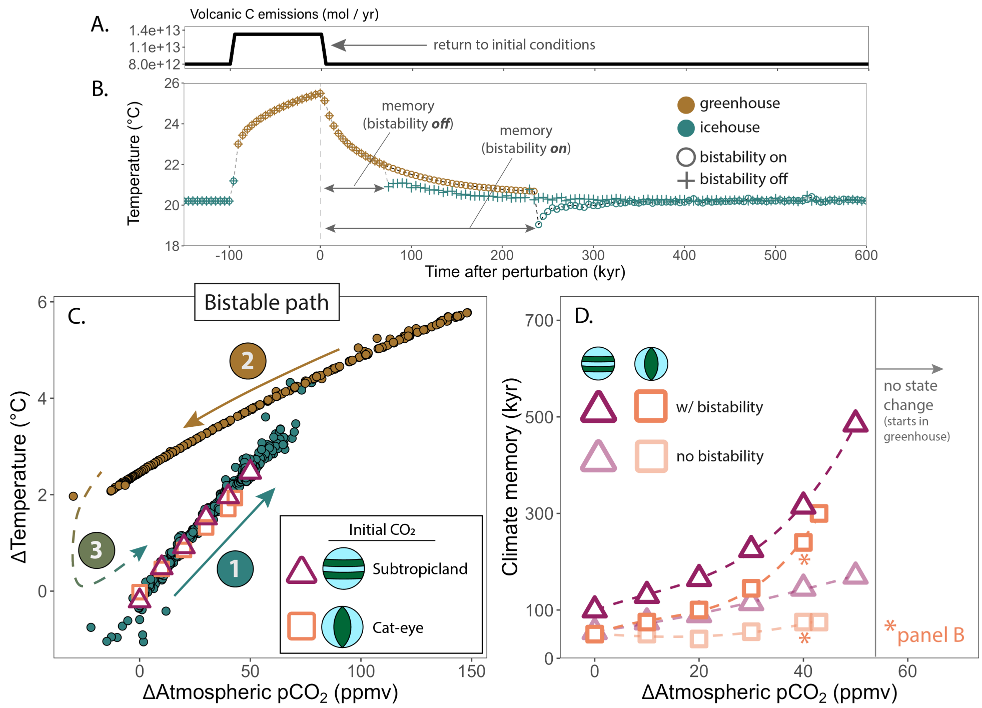

Figure 5. Climate returns to initial state after perturbation. (**A**) Volcanic perturbation for all simulations and (**B**) Example calculation of "memory" using the Cat-eye geography (see asterisk in panel *D*). Note that simulations with and without bistability follow the same path until about 75 kyr after the perturbation ends. (**C**) Small dots show time-transient pCO_2 and temperature results for the Cat-eye simulations (Subtropicland is similar with a temperature offset due to differences in planetary albedo). Larger shapes show the starting conditions for the Cat-eye (orange square) and Subtropicland (purple triangle) geographies. All simulations warm to a greenhouse climate (brown dots) then ultimately return to an icehouse (teal dots). Sparse icehouse points along the greenhouse line are due to the memory effect of the system. (**D**) Memory of the climate system increases in Subtropicland (weaker weathering feedback) and with a higher initial pCO_2, closer to the greenhouse tipping point. In all simulations, the memory of the system is less than 500 kyr. Without bistability, the system recovers faster, especially approaching the icehouse-greenhouse threshold.

4.4 The long-term bistability window

Figure 6A and B show a characteristic experiment constraining the bistability window for a single geography (Midland world) and a single set of climate conditions. The range of pCO_2 values where both icehouse and greenhouse climates are stable in the long-term (*i.e.,* stable to orbital variations) is marked by the gray bracket in Figure 6A. In the absence of long-term carbon cycle constraints, the bracketed bistability window accounts for a $\sim 3°C$ range of global temperatures (light blue rectangle) in this example. However, on million-year timescales, the bistability window is the range of volcanic degassing or weathering flux values (not pCO_2 values) where an icehouse and greenhouse are stable. This long-term bistability window is smaller, spanning 0.3×10^{12} moles of C per year (about 3% of the control simulation degassing rate) and a $\sim 0.5°C$ range in global temperature (Fig. 3B; darker blue rectangles).

The results in panels A and B show a larger long-term bistability window than the majority of climate conditions and continental configurations. About half of all experiments show no long-term bistability, and the bistability window is less than 1×10^{12} moles/yr in all scenarios (Fig. 6C). For reference, volcanic degassing may have varied over the course of the Cenozoic by greater than $4{\times}10^{12}$ moles/yr (Berner, 2006; Caves et al., 2016; Herbert et al., 2022; Van Der Meer et al., 2014). This bistability window further collapses when we assume a lower climate inertia by requiring long-term stable states to be stable for *all* orbital configurations (stable fraction of 1). In this case, two-thirds of all initial conditions have no long-term bistability, and all bistable solutions have a bistablity window smaller than $0.4{\times}10^{12}$ moles/yr (Supplementary Fig. S2). Overall, the long-term bistability window is zero in the majority of our simulations. When a bistability window exists, it is generally limited to a range where volcanic degassing cannot vary by more than a few percent, much less than the variability predicted on million-year timescales (Berner, 2006).

5 Discussion

5.1 Different frameworks for short and long-term climate bistability

A stable climate solution is one that can persist indefinitely; it cannot be reversed by the internal processes nor fixed external forcings on the system. The short and long-term climate systems have different forcings and, therefore, their stability (and bistability) must be evaluated in different frameworks. On sub-million-year timescales where atmospheric pCO_2 is the dominant climate forcing, bistability can be illustrated in a plot of pCO_2 versus global temperature (with temperature serving as a proxy for climate state) (Fig. 6A). This bistability framework breaks down on million-year timescales where climate (and pCO_2 itself) is forced by the balance of CO_2 emissions and sequestration (here, volcanism and weathering). Thus, long-term bistability requires overlap of greenhouse and icehouse states in a plot of temperature against volcanic emissions, not pCO_2 (Fig. 6B).

This long-term bistability framework applies on timescales where the long-term carbon cycle should be considered balanced (generally $< 1-5$ million years to prevent a runaway climate (Berner & Caldeira, 1998; Broecker & Sanyal, 1998; D'Antonio et al., 2020)) such that a given climate state may persist indefinitely. This requirement of a balanced long-term carbon cycle ultimately restricts the long-term bistability window due to the effect of the negative silicate weathering feedback. A balanced long-term carbon cycle requires that icehouse and greenhouse states have the same weathering flux to balance volcanism, and this condition is generally met when the greenhouse pCO_2 level is lower than the alternate icehouse state, thereby compensating for the lower albedo of the ice-free greenhouse and resulting in similar global temperatures, runoff, and weathering fluxes for each state. Importantly, there is only a small range of conditions where

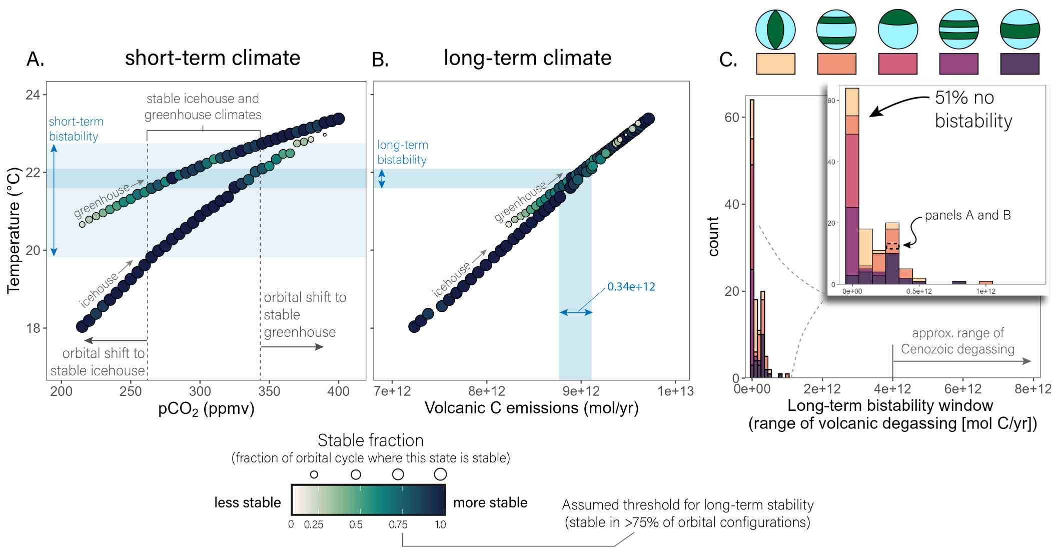

Figure 6. A limited long-term bistability window. Characteristic results showing the short-term (**A**) and long-term (**B**) bistability frameworks with pCO_2 and volcanism as the forcings, respectively, for a single set of internal parameters in the Midland world. Point size and color refers to the stability of a given climate solution, calculated as the fraction of orbital configurations where the state is stable. (**C**) There is no long-term bistability in 53% of simulations (from a range of geographies and climate conditions; inset), and the simulations that produce long-term bistability yield a small bistability window compared to changes in volcanic degassing. This bistability window is generally limited to a volcanic degassing range of $< 0.5 \times 10^{12}$ moles C/yr, or within $\sim 6\%$ of modern degassing.

a greenhouse is stable at a lower pCO_2 than an icehouse, and these solutions occur near the upper and lower-bounds of the short-term bistability window (close to the icehouse-greenhouse tipping points). This effect can be seen in Fig. 6A where the temperature range for long-term bistability (darker blue horizontal bar) overlaps with the low-pCO_2 stable greenhouse states, the high-pCO_2 stable icehouse states, but not the climate states in between. The core of the short-term bistability window is not bistable in the long-term climate.

The fact that the long-term bistability window mostly exists near the icehouse-greenhouse tipping points explains why this bistability window is so sensitive to "noise" or internal variability such as orbital cycles. When the climate state is near a tipping point, internal variability is more likely to nudge the system to the new, often more stable, state. In Figure 6A, for example, the low-pCO_2 greenhouse is less stable than the icehouse climate at the same pCO_2 such that internal variability will favor tipping from the greenhouse to the more stable icehouse. It is likely that our simulations underestimate the true internal variability of the climate system because (1) we do not account for seasonal effects that can amplify the effect of orbital variability on climate and (2) we impose a conservatively high climate inertia, so the model tends to stay in the same climate state even as that climate state becomes increasingly unstable. Consequently, we are likely overestimating the range of volcanic degassing variations where long-term bistability is reasonable (Fig. 6C).

5.2 Implications for paleoclimate transitions

Our results emphasize that the climate system can be bistable in the short-term *and* deterministic on million-year timescales—one does not exclude the other—a finding that contradicts previous conceptual models based on inherently short-term frameworks (DeConto & Pollard, 2003; Hyde et al., 1999; Kypke & Langford, 2020; Murante et al., 2020; Pohl et al., 2014; Stap et al., 2017). Consider, for example, a transition from a greenhouse climate to an icehouse climate with a lower global temperature but the same atmospheric pCO_2. In the short-term, these two states are bistable because pCO_2 is the dominant forcing on the system. In the long-term, however, lower weathering fluxes in the cooler, icehouse state require decreased volcanism or a more reactive land surface to balance the carbon cycle (*e.g.* Caves Rugenstein et al. (2019); Kump and Arthur (1997); Lear et al. (2004)). If volcanism does not decrease or land surface reactivity does not increase, CO_2 will accumulate in the atmosphere and the greenhouse state will be restored. Short-term bistability therefore collapses in the long-term (Fig. 6). The greenhouse-icehouse transition must be forced by (or at least coincident with) some change in volcanism, weathering, or other endogenic carbon flux, thereby making the climate state deterministic; otherwise the new icehouse is unlikely to persist.

The above thought experiment applies to the Cenozoic example we discussed in section 2. Some pCO_2 reconstructions for the Cenozoic imply a bistable climate (see Fig. 1B) with an icehouse-greenhouse transition that occurred ~ 34 million years ago across the Eocene-Oligocene boundary. Much work has sought to explain this transition in terms of passing a critical pCO_2 threshold (DeConto & Pollard, 2003; DeConto et al., 2008; Gasson et al., 2014; Goldner et al., 2014; Pearson et al., 2009; Stap et al., 2017). These analyses are appropriate for explaining the abrupt nature of the transition, but they do not address why the icehouse state persisted for millions of years (Lear et al., 2004). Other studies invoke the long-term carbon cycle as the external forcing, more directly addressing the persistence of the icehouse (Caves et al., 2016; Elsworth et al., 2017; Lear et al., 2004; Lefebvre et al., 2013; Scher et al., 2011), but are limited in their ability to address the role of positive climate feedbacks in driving the icehouse transition and its abruptness. In contrast, Pollard et al. (2013) combine an ice sheet model that exhibits multistability with different weathering formulations to resolve the abruptness and persistence of the Eocene-Oligocene transition. Their findings are consistent with our results—a long-term carbon cycle forcing (in their case, a decrease in volcanism) is needed for the new icehouse state to persist, making the global climate state deterministic.

The multi-million year persistence of icehouse or greenhouse climates in the Cenozoic are perhaps an obvious and relatively well-constrained test of deterministic, "long-term" climate states, but on what timescales does this "long-term" determinism apply? Since long-term bistability depends on a balanced carbon cycle (as discussed above), long-term bistability is restricted to longer timescales when the recovery time of the carbon cycle is slow. A weak silicate weathering feedback, for example, will allow the carbon cycle to remain imbalanced longer, extending the window in which the "short-term" bistability framework applies. Similarly, carbon cycle imbalances can be extremely prolonged in "Snowball Earth" climates—times of near-total Earth glaciation that are often considered a bistable climate solution. Snowball Earth events can last many millions of years, during which ice cover restricts weathering, leading to excess volcanic C emissions and keeping the long-term carbon cycle out of balance (Walker et al., 1981; Hoffman et al., 2017). As a result, snowball climates are akin to the short-lived icehouse-greenhouse bistability in our simulations (see Fig. 5B)—their existence is reversible and limited by the time required for the carbon cycle to restore balance. Snowball irreversibility is theoretically possible, but implausible for at least the most recent, Neoproterozoic snowball events (Turbet, 2017). Their more sluggish carbon cycle recovery means that snowball states meet the conditions for short-term bistability (irreversible when the long-term carbon cycle is ignored) for a longer window of time than their alternative, stable ice-free states.

That recovery times are variable, even for a single planet, is a critical consideration for identifying habitable exoplanets. Murante et al. (2020), for example, use an energy balance model to argue that the same conditions that support a snowball can also support a climate warm enough for liquid water and therefore life. We add that, in much the same way that the long-term climate state cannot be fully determined on short timescales in our model simulations, the co-existence of a habitable state and a snowball in an energy balance model does not imply that the habitable state will persist once it is realized. The persistence of a habitable state in a bistable snowball planet will depend on the greenhouse gas (or radiative) forcing level at which the long-term carbon cycle is balanced after the snowball melts (Abbot et al., 2012; Graham & Pierrehumbert, 2020).

5.3 Diagnosing icehouse-greenhouse bistability with empirical evidence

Snowball Earth states aside, our model indicates that the global climate state on million-year timescales is likely deterministic. How then do we explain apparent bistability on these timescales in the Cenozoic? And how can paleoclimate timeseries data be used to test for climate bistability?

There are two primary ways in which multi-million year climate data can appear bistable (see Fig. 1B) without requiring a long-term, bistable climate. In the first case, short-term bistability exists in the climate system, but long-term forcings are necessary to navigate this bistability landscape. These forcings make the long-term climate state deterministic—a greenhouse requires more volcanism than an icehouse, even for the same pCO_2. In the second case, internal system parameters that can change independently from climate (including geography, ocean heat transport, land albedo, and radiative feedback strengths) change the equilibrium temperature for a given pCO_2 level, creating the appearance of bistability driven by changes in global temperature that do not necessarily depend on pCO_2. This second option, changes in internal system parameters, must be ruled out to confidently diagnose short-term climate bistability from long-term temperature and pCO_2 data. How to rule out such a myriad of processes is beyond the scope of this paper, although efforts to constrain the maximum possible climate impacts of the major internal processes are a useful step toward this goal.

However, analyzing paleoclimate data on shorter timescales, where we need not assume a balanced carbon cycle, is a more direct test of short-term climate bistability. Although not strictly icehouse-greenhouse bistability, analysis of $\sim$ 100kyr glacial-interglacial cycles has long centered around the possibility that they represent distinct climate states (Ferreira et al., 2018; Hyde et al., 1999; Vettoretti et al., 2022). In the middle Miocene, Foster et al. (2012) test for evidence of memory effects (hysteresis) in temperature and pCO_2 proxy data collected at $\sim$ 300kyr resolution. The lack of hysteresis in their data was used to suggest that sea ice, thought to show much less hysteresis than land ice (Pollard & DeConto, 2009), was the primary driver of climate and sea level (Foster et al., 2012). We note, however, that their average sampling resolution is likely longer than the recovery time of the carbon cycle in the mid-Miocene (Penman et al., 2020). Any bistability and hysteresis would likely collapse on these timescales, making it harder to detect with their data resolution. Subsequent work produced a higher resolution record with no clear evidence for hysteresis (Greenop et al., 2014). Indeed, the long-term carbon cycle should restrict the duration of bistability in ice sheet models as well, so long as ice albedo feeds back on global climate. If ice coverage is primarily driven by the height mass balance feedback (ice sheet growth causes more precipitation and thus ice sheet growth; (Abe-Ouchi & Blatter, 1993; Birchfield et al., 1982; DeConto & Pollard, 2003; Morales Maqueda et al., 1998; Pollard & DeConto, 2005)), with no effect on global climate, then we expect the long-term carbon cycle will have less of an effect on ice sheet bistability. However, we are not aware of any research that has tested the response of long-term ice sheet memory to ice albedo and height mass balance feedbacks with a coupled long-term carbon cycle model.

5.4 Limitations of model framework

Whether our model results accurately represent the determinism of long-term climate hinges on (1) a non-linear positive feedback linking CO_2 (or radiative forcing) to global temperature; (2) a negative feedback that stabilizes global temperature on million-year timescales; and (3) the lack of any bistability (or multi-stability) inherent to the long-term carbon cycle.

In our model, the ice albedo feedback is the non-linear positive feedback that permits short-term bistability. However, the effect of ice albedo on global climate has recently been called into question (Datseris & Stevens, 2021). The lack of a feedback between ice albedo and global temperature would likely lead to a more deterministic short-term (and thus long-term) climate. Other non-linear positive feedbacks not represented in our model, such as the possible loss of subtropical stratocumulus clouds with warming, may also cause climate bistability (Schneider et al., 2019). However, this too should be short-lived because the low- and high-cloud states represent different global temperatures and therefore likely different weathering fluxes. In short, for any non-linear positive radiative feedback, a long-term negative feedback that stabilizes climate would tend to act against it, limiting the positive feedback's potential to cause bistability in the long-term.

We use the silicate weathering feedback to represent the long-term negative feedback in our model, but the strength of this feedback now and throughout Earth history is not well known (Penman et al., 2020). Some modeling work has suggested scenarios where this negative feedback breaks down (Pollard et al., 2013; Kump, 2018), in which case the climate system is likely to runaway or perhaps exhibit multiple stable states (Mills et al., 2021). Our model finds a robust weathering feedback largely because the runoff response to pCO_2 is positive in nearly all cases, and generally consistent with the runoff response in more complex, Earth System Models (X. Zhang et al., 2014). Other negative feedbacks may also be important for long-term carbon sequestration, such as the erosion-driven export of terrestrial organic carbon (Hilton & West, 2020). However, most important to our conclusions is that a negative feedback on long-term climate exists. One of the strongest lines of evidence commonly evoked for a negative long-term climate feedback is that our planet has been habitable for more than four billion years, and it takes less than 10 million years for a 5% imbalance in greenhouse gas emissions versus sequestration to manifest as a runaway climate (Berner & Caldeira, 1998; Broecker & Sanyal, 1998). Whether due to silicate weathering or some other biogeochemical processes, a negative feedback on long-term climate will act to collapse long-term bistability.

Finally, a deterministic climate on million-year timescales requires a lack of non-linear, positive feedbacks in the long-term carbon cycle that can cause bistability. Positive feedbacks have been proposed (*e.g.*, Mills et al. (2021)), but are not yet well-tested nor widely accepted. Recently, Mills et al. (2021) suggested that tropical weathering rates could decrease with warming, causing net CO_2 emissions until climate is warm enough for increases in mid-latitude weathering to balance the losses in the tropics. As a result, they simulate more than one global temperature for a given volcanic degassing rate—fitting the criteria for climate bistability in the long-term framework (Fig. 6B). However, their model is a preliminary proof of concept for carbon cycle multi-stability, and more work is needed to verify the tight coupling between tropical plant productivity and weathering that is proposed. Our model does not include any processes that can replicate this effect, although a strong enough positive carbon cycle feedback should cause long-term bistability in our model as well. Addressing the plausibility of such positive feedbacks is an important next step in constraining how deterministic the global climate system is on million-year timescales.

6 Conclusion

There is mounting evidence from the geologic past that icehouse-greenhouse transitions spanning millions of years are driven by the balance of weathering and volcanism (Caves et al., 2016; Dalton et al., 2022; Herbert et al., 2022; McKenzie et al., 2016; McKenzie & Jiang, 2019), rather than irreversible nudges across a critical threshold (Pohl et al., 2014; Stap et al., 2017). Our analysis strengthens the theoretical foundation underlying this empirical evidence for a deterministic long-term climate. A negative long-term climate feedback will limit, if not collapse, any bistability that emerges from a nonlinear positive radiative feedback, regardless of what these feedbacks are. While the timescale for collapsing bistability is longer in a Snowball Earth state or when the silicate weathering feedback is weak, bistable states remain generally reversible—the memory of the climate system is finite. The ability of the long-term negative feedback to limit bistability depends on the range of temperatures (or weathering fluxes) in which both climate states can exist. This range is limited by internal noise such as orbital forcing, and it is rather small and fragile for a wide array of input parameter values. Notwithstanding positive feedbacks in the long-term carbon cycle that remain speculative, our results cast Earth's climate system as highly deterministic on million-year timescales.

Acknowledgments

We are grateful for constructive conversations with Sandra Schachat and Keno Reichers that improved this manuscript. We also acknowledge Thomas Westerhold for sharing the pCO_2 compilation used in Figure 1B.

References

Abbot, D. S., Cowan, N. B., & Ciesla, F. J. (2012, September). Indication of insensitivity of planetary weathering behavior and habitable zone to surface land fraction. *The Astrophysical Journal*, *756*(2), 178. doi: 10.1088/0004-637X/756/2/178

Abbot, D. S., Voigt, A., & Koll, D. (2011, September). The Jormungand global climate state and implications for Neoproterozoic glaciations. *Journal of Geophysical Research*, *116*(D18), D18103. doi: 10.1029/2011JD015927

Abe-Ouchi, A., & Blatter, H. (1993). On the initiation of ice sheets. *Annals of Glaciology*, *18*, 203–207. doi: 10.3189/S0260305500011514

Archer, D. (2005). Fate of fossil fuel CO $_2$ in geologic time. *Journal of Geophysical Research*, *110*(C9), C09S05. doi: 10.1029/2004JC002625

Bachan, A., & Kump, L. R. (2015, May). The rise of oxygen and siderite oxidation during the Lomagundi Event. *Proceedings of the National Academy of Sciences*, *112*(21), 6562–6567. doi: 10.1073/pnas.1422319112

Berger, A. (1978). Long-term variations of daily insolation and Quaternary climatic changes. *Journal of the Atmospheric Sciences*, *35*, 2362–2367.

Berger, A., Loutre, M.-F., & Yin, Q. (2010, August). Total irradiation during any time interval of the year using elliptic integrals. *Quaternary Science Reviews*, *29*(17-18), 1968–1982. doi: 10.1016/j.quascirev.2010.05.007

Berner, R. A. (1991). A model for atmospheric CO2 over Phanerozoic time. *American Journal of Science*, *291*, 339–376. doi: 10.2475/ajs.291.4.339

Berner, R. A. (2004). *The Phanerozoic Carbon Cycle: CO2 and O2.* New York: Oxford University Press.

Berner, R. A. (2006). GEOCARBSULF: A combined model for Phanerozoic atmospheric O2 and CO2. *Geochimica et Cosmochimica Acta*, *70*(23 SPEC. ISS.), 5653–5664. doi: 10.1016/j.gca.2005.11.032

Berner, R. A., & Caldeira, K. (1998). The need for mass balance and feedback in the geochemical carbon cycle: Comment and Reply. *Geology*, *26*(5), 478. doi: 10.1130/0091-7613(1998)026⟨0477:TNFMBA⟩2.3.CO;2

Birchfield, G. E., Weertman, J., & Lunde, A. T. (1982, January). A Model Study of the Role of High-Latitude Topography in the Climatic Response to Orbital Insolation Anomalies. *Journal of the Atmospheric Sciences*, *39*(1), 71–87. doi: 10.1175/1520-0469(1982)039⟨0071:AMSOTR⟩2.0.CO;2

Bluth, G. J. S., & Kump, L. R. (1994). Lithologic and climatologic controls of river chemistry. *Geochimica et Cosmochimica Acta*, *58*(10), 2341–2359. doi: 10.1016/0016-7037(94)90015-9

Borchers, H. W. (2021). *Pracma: Practical Numerical Math Functions.*

Broecker, W. S., & Sanyal, A. (1998, September). Does atmospheric CO $_2$ police the rate of chemical weathering? *Global Biogeochemical Cycles*, *12*(3), 403–408. doi: 10.1029/98GB01927

Budyko, M. I. (1969, October). The effect of solar radiation variations on the climate of the Earth. *Tellus*, *21*(5), 611–619. doi: 10.1111/j.2153-3490.1969.tb00466.x

Budyko, M. I. (1974). *Climate and Life. International Geophysical Series, Vol. 18* (Vol. 18). Academic Press.

Burls, N. J., & Fedorov, A. V. (2017). Wetter subtropics in a warmer world : Contrasting past and future hydrological cycles. *Proceedings of the National Academy of Sciences*, *114*(49). doi: 10.1073/pnas.1703421114

Byrne, M. P., & O'Gorman, P. A. (2015). The Response of Precipitation Minus Evapotranspiration to Climate Warming : Why the "Wet-Get-Wetter, Dry-Get-Drier" Scaling Does Not Hold over Land*. *Journal of Climate*, 8078–8092. doi: 10.1175/JCLI-D-15-0369.1

Caves, J. K., Jost, A. B., Lau, K. V., & Maher, K. (2016). Cenozoic carbon cycle imbalances and a variable weathering feedback. *Earth and Planetary Science Letters*, *450*, 152–163. doi: 10.1016/j.epsl.2016.06.035

Caves Rugenstein, J. K., Ibarra, D. E., & von Blanckenburg, F. (2019, July). Neogene cooling driven by land surface reactivity rather than increased weathering fluxes. *Nature*, *571*(7763), 99–102. doi: 10.1038/s41586-019-1332-y

Crucifix, M. (2016). *Palinsol: Insolation for Paleoclimate Studies.*

Dalton, C. A., Wilson, D. S., & Herbert, T. D. (2022, March). Evidence for a Global Slowdown in Seafloor Spreading Since 15 Ma. *Geophysical Research Letters*, *49*(6). doi: 10.1029/2022GL097937

D'Antonio, M. P., Ibarra, D. E., & Boyce, C. K. (2020, January). Land plant evolution decreased, rather than increased, weathering rates. *Geology*, *48*(1), 29–33. doi: 10.1130/G46776.1

Datseris, G., & Stevens, B. (2021, September). Earth's Albedo and Its Symmetry. *AGU Advances*, *2*(3). doi: 10.1029/2021AV000440

DeConto, R. M., & Pollard, D. (2003, January). Rapid Cenozoic glaciation of Antarctica induced by declining atmospheric CO2. *Nature*, *421*(6920), 245–249. doi: 10.1038/nature01290

DeConto, R. M., Pollard, D., Wilson, P. A., Pälike, H., Lear, C. H., & Pagani, M. (2008, October). Thresholds for Cenozoic bipolar glaciation. *Nature*, *455*(7213), 652–656. doi: 10.1038/nature07337

De Vleeschouwer, D., Drury, A. J., Vahlenkamp, M., Rochholz, F., Liebrand, D., & Pälike, H. (2020, December). High-latitude biomes and rock weathering mediate climate–carbon cycle feedbacks on eccentricity timescales. *Nature Communications*, *11*(1), 5013. doi: 10.1038/s41467-020-18733-w

Dortmans, B., Langford, W. F., & Willms, A. R. (2019, March). An energy balance model for paleoclimate transitions. *Climate of the Past*, *15*(2), 493–520. doi: 10.5194/cp-15-493-2019

Elsworth, G., Galbraith, E., Halverson, G., & Yang, S. (2017). Enhanced weathering and CO2 drawdown caused by latest Eocene strengthening of the Atlantic meridional overturning circulation. *Nature Geoscience*(January). doi: 10.1038/ngeo2888

Ferreira, D., Marshall, J., Ito, T., & McGee, D. (2018, September). Linking Glacial-Interglacial States to Multiple Equilibria of Climate. *Geophysical Research Letters*, *45*(17), 9160–9170. doi: 10.1029/2018GL077019

Ferreira, D., Marshall, J., & Rose, B. (2011, February). Climate Determinism Revisited: Multiple Equilibria in a Complex Climate Model. *Journal of Climate*, *24*(4), 992–1012. doi: 10.1175/2010JCLI3580.1

Flannery, B. P. (1984). Energy Balance Models Incorporating Transport of Thermal and Latent Energy. *Journal of Atmospheric Sciences*, *41*(3), 414–421. doi: 10.1175/1520-0469(1984)041⟨0414:EBMITO⟩2.0.CO;2

Foster, G. L., Lear, C. H., & Rae, J. W. (2012, August). The evolution of pCO2, ice volume and climate during the middle Miocene. *Earth and Planetary Science Letters*, *341–344*, 243–254. doi: 10.1016/j.epsl.2012.06.007

Foster, G. L., & Rohling, E. J. (2013, January). Relationship between sea level and climate forcing by CO_2 on geological timescales. *Proceedings of the National Academy of Sciences*, *110*(4), 1209–1214. doi: 10.1073/pnas.1216073110

Frierson, D. M. W., Held, I. M., & Zurita-Gotor, P. (2006). A Gray-Radiation Aquaplanet Moist GCM. Part II: Energy Transports in Altered Climates. *Journal of the Atmospheric Sciences*, *64*(5), 1680–1693. doi: 10.1175/JAS3913.1

Fu, B. P. (1981). On the calculation of the evaporation from land surface. *Sci. Atmos. Sin*, *5*(1), 23–31.

Gasson, E., Lunt, D. J., DeConto, R., Goldner, A., Heinemann, M., Huber, M., … Valdes, P. J. (2014, March). Uncertainties in the modelled CO₂ threshold for Antarctic glaciation. *Climate of the Past*, *10*(2), 451–466. doi: 10.5194/cp-10-451-2014

Goldner, A., Herold, N., & Huber, M. (2014, July). Antarctic glaciation caused ocean circulation changes at the Eocene–Oligocene transition. *Nature*, *511*(7511), 574–577. doi: 10.1038/nature13597

Gosling, W. D., & Holden, P. B. (2011, July). Precessional forcing of tropical vegetation carbon storage. *Journal of Quaternary Science*, *26*(5), 463–467. doi: 10.1002/jqs.1514

Graham, R. J. (2021, November). High pCO_2 Reduces Sensitivity to CO_2 Perturbations on Temperate, Earth-like Planets Throughout Most of Habitable Zone. *Astrobiology*, *21*(11), 1406–1420. doi: 10.1089/ast.2020.2411

Graham, R. J., & Pierrehumbert, R. (2020, June). Thermodynamic and Energetic Limits on Continental Silicate Weathering Strongly Impact the Climate and Habitability of Wet, Rocky Worlds. *The Astrophysical Journal*, *896*(2), 115. doi: 10.3847/1538-4357/ab9362

Greenop, R., Foster, G. L., Wilson, P. A., & Lear, C. H. (2014, September). Middle Miocene climate instability associated with high-amplitude CO_2 variability: Large variability in Middle Miocene CO2. *Paleoceanography*, *29*(9), 845–853. doi: 10.1002/2014PA002653

Greve, P., Gudmundsson, L., Orlowsky, B., & Seneviratne, S. I. (2015). Introducing a probabilistic Budyko framework. *Geophysical Research Letters*, *42*(7), 2261–2269. doi: 10.1002/2015GL063449

Herbert, T. D., Dalton, C. A., Liu, Z., Salazar, A., Si, W., & Wilson, D. S. (2022, July). Tectonic degassing drove global temperature trends since 20 Ma. *Science*, *377*(6601), 116–119. doi: 10.1126/science.abl4353

Hilton, R. G., & West, A. J. (2020, June). Mountains, erosion and the carbon cycle. *Nature Reviews Earth & Environment*, *1*(6), 284–299. doi: 10.1038/s43017-020-0058-6

Hoffman, P. F., Abbot, D. S., Ashkenazy, Y., Benn, D. I., Brocks, J. J., Cohen, P. A., … Warren, S. G. (2017, November). Snowball Earth climate dynamics and Cryogenian geology-geobiology. *Science Advances*, *3*(11), e1600983. doi: 10.1126/sciadv.1600983

Hwang, Y. T., & Frierson, D. M. (2010). Increasing atmospheric poleward energy

transport with global warming. *Geophysical Research Letters*, *37*(24), 1–5. doi: 10.1029/2010GL045440
Hyde, W. T., Crowley, T. J., Tarasov, L., & Peltier, W. R. (1999, September). The Pangean ice age: Studies with a coupled climate-ice sheet model. *Climate Dynamics*, *15*(9), 619–629. doi: 10.1007/s003820050305
Ibarra, D. E., Caves, J. K., Moon, S., Thomas, D. L., Hartmann, J., Chamberlain, C. P., & Maher, K. (2016). Differential weathering of basaltic and granitic catchments from concentration-discharge relationships. *Geochimica et Cosmochimica Acta*, *190*, 265–293. doi: 10.1016/j.gca.2016.07.006
Isson, T. T., Planavsky, N. J., Coogan, L. A., Stewart, E. M., Ague, J. J., Bolton, E. W., ... Kump, L. R. (2020, February). Evolution of the Global Carbon Cycle and Climate Regulation on Earth. *Global Biogeochemical Cycles*, *34*(2). doi: 10.1029/2018GB006061
Jagoutz, O., Macdonald, F. A., & Royden, L. (2016, May). Low-latitude arc–continent collision as a driver for global cooling. *Proceedings of the National Academy of Sciences*, *113*(18), 4935–4940. doi: 10.1073/pnas.1523667113
Kasting, J. F. (1993). Earth's Early Atmosphere. *Science*, *259*(5097), 920–926.
Knutti, R., Rugenstein, M. A. A., & Hegerl, G. C. (2017). Beyond equilibrium climate sensitivity. *Nature Geoscience*(September). doi: 10.1038/ngeo3017
Koll, D. D. B., & Cronin, T. W. (2018, October). Earth's outgoing longwave radiation linear due to H $_2$ O greenhouse effect. *Proceedings of the National Academy of Sciences*, *115*(41), 10293–10298. doi: 10.1073/pnas.1809868115
Krissansen-Totton, J., & Catling, D. C. (2017, August). Constraining climate sensitivity and continental versus seafloor weathering using an inverse geological carbon cycle model. *Nature Communications*, *8*(1), 15423. doi: 10.1038/ncomms15423
Kukla, T., Ibarra, D., Lau, K., & Rugenstein, J. (2022a, September). *All aboard! Earth system investigations with the CH2O-CHOO TRAIN v1.0* (Preprint). EarthArXiv. doi: 10.31223/X5ND26
Kukla, T., Ibarra, D., Lau, K., & Rugenstein, J. K. C. (2022b). Project files, data, and code. *Zenodo*. doi: 10.5281/zenodo.7072803
Kump, L. R. (2018, October). Prolonged Late Permian–Early Triassic hyperthermal: Failure of climate regulation? *Philosophical Transactions of the Royal Society A: Mathematical, Physical and Engineering Sciences*, *376*(2130), 20170078. doi: 10.1098/rsta.2017.0078
Kump, L. R., & Arthur, M. A. (1997). Global Chemical Erosion during the Cenozoic: Weatherability Balances the Budgets. In *Tectonic uplift and climate change* (pp. 399–426). doi: 10.1007/978-1-4615-5935-1
Kypke, K. L., & Langford, W. F. (2020, February). Topological Climate Change. *International Journal of Bifurcation and Chaos*, *30*(02), 2030005. doi: 10.1142/S0218127420300050
Laguë, M. M., Pietschnig, M., Ragen, S., Smith, T. A., & Battisti, D. S. (2021). Terrestrial Evaporation and Global Climate: Lessons from Northland, a Planet with a Hemispheric Continent. *Journal of Climate*, *34*, 24.
Laskar, J., Robutel, P., Joutel, F., Gastineau, M., Correia, A. C. M., & Levrard, B. (2004, December). A long-term numerical solution for the insolation quantities of the Earth. *Astronomy & Astrophysics*, *428*(1), 261–285. doi: 10.1051/0004-6361:20041335
Lear, C. H., Rosenthal, Y., Coxall, H. K., & Wilson, P. A. (2004, December). Late Eocene to early Miocene ice sheet dynamics and the global carbon cycle: EOCENE TO MIOCENE ICE SHEET DYNAMICS. *Paleoceanography*, *19*(4), n/a-n/a. doi: 10.1029/2004PA001039
Lee, C. T. A., Shen, B., Slotnick, B. S., Liao, K., Dickens, G. R., Yokoyama, Y., ... Tice, M. M. (2013). Continental arc-island arc fluctuations, growth of

crustal carbonates, and long-term climate change. *Geosphere*, *9*(1), 21–36. doi: 10.1130/GES00822.1

Lefebvre, V., Donnadieu, Y., Goddéris, Y., Fluteau, F., & Hubert-Théou, L. (2013, June). Was the Antarctic glaciation delayed by a high degassing rate during the early Cenozoic? *Earth and Planetary Science Letters*, *371–372*, 203–211. doi: 10.1016/j.epsl.2013.03.049

Lisiecki, L. E., & Raymo, M. E. (2005, March). A Pliocene-Pleistocene stack of 57 globally distributed benthic δ ^{18} O records: PLIOCENE-PLEISTOCENE BENTHIC STACK. *Paleoceanography*, *20*(1), n/a-n/a. doi: 10.1029/2004PA001071

Macdonald, F. A., Swanson-Hysell, N. L., Park, Y., Lisiecki, L., & Jagoutz, O. (2019, April). Arc-continent collisions in the tropics set Earth's climate state. *Science*, *364*(6436), 181–184. doi: 10.1126/science.aav5300

Maher, K. (2011). The role of fluid residence time and topographic scales in determining chemical fluxes from landscapes. *Earth and Planetary Science Letters*, *312*(1-2), 48–58. doi: 10.1016/j.epsl.2011.09.040

Maher, K., & Chamberlain, C. P. (2014). Hydrologic regulation of chemical weathering and the geologic carbon cycle. *Science (New York, N.Y.)*, *343*(6178), 1502–4. doi: 10.1126/science.1250770

Mazzia, F., Cash, J. R., & Soetaert, K. (2014). Solving boundary value problems in the open source software R: Package bvpSolve. *Opuscula mathematica*, *34*(2), 387–403.

McKenzie, N. R., Horton, B. K., Loomis, S. E., Stockli, D. F., Planavsky, N. J., & Lee, C.-T. A. (2016). Continental arc volcanism as the principal driver of icehouse-greenhouse variability. *Science*, *352*(6284), 444–447. doi: 10.1126/science.aad5787

McKenzie, N. R., & Jiang, H. (2019, October). Earth's Outgassing and Climatic Transitions: The Slow Burn Towards Environmental "Catastrophes"? *Elements*, *15*(5), 325–330. doi: 10.2138/gselements.15.5.325

Mills, B. J. W., Tennenbaum, S., & Schwartzman, D. (2021, September). Exploring multiple steady states in Earth's long-term carbon cycle. *American Journal of Science*, *321*(7), 1033–1044. doi: 10.2475/07.2021.01

Morales Maqueda, M. A., Willmott, A. J., Bamber, J. L., & Darby, M. S. (1998, April). An investigation of the small ice cap instability in the Southern Hemisphere with a coupled atmosphere-sea ice-ocean-terrestrial ice model. *Climate Dynamics*, *14*(5), 329–352. doi: 10.1007/s003820050227

Murante, G., Provenzale, A., Vladilo, G., Taffoni, G., Silva, L., Palazzi, E., … Zorba, S. (2020, February). Climate bistability of Earth-like exoplanets. *Monthly Notices of the Royal Astronomical Society*, *492*(2), 2638–2650. doi: 10.1093/mnras/stz3529

North, G. R., Cahalan, R. F., & Coakley, J. A. (1981). Energy Balance Climate Models. *Reviews of Geophysics and Space Physics*, *19*(1), 91–121. doi: 10.1029/RG019i001p00091

Park, Y., Maffre, P., Goddéris, Y., Macdonald, F. A., Anttila, E. S. C., & Swanson-Hysell, N. L. (2020, October). Emergence of the Southeast Asian islands as a driver for Neogene cooling. *Proceedings of the National Academy of Sciences*, *117*(41), 25319–25326. doi: 10.1073/pnas.2011033117

Pearson, P. N., Foster, G. L., & Wade, B. S. (2009, October). Atmospheric carbon dioxide through the Eocene–Oligocene climate transition. *Nature*, *461*(7267), 1110–1113. doi: 10.1038/nature08447

Penman, D. E., Caves Rugenstein, J. K., Ibarra, D. E., & Winnick, M. J. (2020, October). Silicate weathering as a feedback and forcing in Earth's climate and carbon cycle. *Earth-Science Reviews*, *209*, 103298. doi: 10.1016/j.earscirev.2020.103298

Pohl, A., Donnadieu, Y., Le Hir, G., Buoncristiani, J.-F., & Vennin, E. (2014, November). Effect of the Ordovician paleogeography on the (in)stability of the climate. *Climate of the Past*, *10*(6), 2053–2066. doi: 10.5194/cp-10-2053-2014

Pollard, D., & DeConto, R. M. (2005, February). Hysteresis in Cenozoic Antarctic ice-sheet variations. *Global and Planetary Change*, *45*(1-3), 9–21. doi: 10.1016/j.gloplacha.2004.09.011

Pollard, D., & DeConto, R. M. (2009, March). Modelling West Antarctic ice sheet growth and collapse through the past five million years. *Nature*, *458*(7236), 329–332. doi: 10.1038/nature07809

Pollard, D., Kump, L., & Zachos, J. (2013, December). Interactions between carbon dioxide, climate, weathering, and the Antarctic ice sheet in the earliest Oligocene. *Global and Planetary Change*, *111*, 258–267. doi: 10.1016/j.gloplacha.2013.09.012

Rae, J. W., Zhang, Y. G., Liu, X., Foster, G. L., Stoll, H. M., & Whiteford, R. D. (2021, May). Atmospheric CO_2 over the Past 66 Million Years from Marine Archives. *Annual Review of Earth and Planetary Sciences*, *49*(1), 609–641. doi: 10.1146/annurev-earth-082420-063026

Raymo, M., & Ruddiman, W. F. (1992). Tectonic Forcing of Late Cenozoic Climate. *Nature*.

Ridgwell, A. J. (2003, June). An end to the "rain ratio" reign? *Geochemistry, Geophysics, Geosystems*, *4*(6), n/a-n/a. doi: 10.1029/2003GC000512

Roe, G. H., Feldl, N., Armour, K. C., Hwang, Y.-t., & Frierson, D. M. W. (2015). The remote impacts of climate feedbacks on regional climate predictability. *Nature Geoscience*, *8*(January). doi: 10.1038/NGEO2346

Rose, B. E. J., Armour, K. C., Battisti, D. S., Feldl, N., & Koll, D. D. B. (2014, February). The dependence of transient climate sensitivity and radiative feedbacks on the spatial pattern of ocean heat uptake. *Geophysical Research Letters*, *41*(3), 1071–1078. doi: 10.1002/2013GL058955

Rose, B. E. J., Cronin, T. W., & Bitz, C. M. (2017, August). Ice Caps and Ice Belts: The Effects of Obliquity on Ice-Albedo Feedback. *The Astrophysical Journal*, *846*(1), 28. doi: 10.3847/1538-4357/aa8306

Rose, B. E. J., & Marshall, J. (2009, September). Ocean Heat Transport, Sea Ice, and Multiple Climate States: Insights from Energy Balance Models. *Journal of the Atmospheric Sciences*, *66*(9), 2828–2843. doi: 10.1175/2009JAS3039.1

Rugenstein, J. K. C., Ibarra, D. E., Zhang, S., Planavsky, N. J., & von Blanckenburg, F. (2021, July). Isotope mass-balance constraints preclude that mafic weathering drove Neogene cooling. *Proceedings of the National Academy of Sciences*, *118*(30), e2026345118. doi: 10.1073/pnas.2026345118

Sagan, C., & Mullen, G. (1972). Earth and Mars: Evolution of Atmospheres and Surface Temperatures. *Science*, *177*, 52–56.

Scher, H. D., Bohaty, S. M., Zachos, J. C., & Delaney, M. L. (2011, April). Two-stepping into the icehouse: East Antarctic weathering during progressive ice-sheet expansion at the Eocene–Oligocene transition. *Geology*, *39*(4), 383–386. doi: 10.1130/G31726.1

Schneider, T., Kaul, C. M., & Pressel, K. G. (2019, March). Possible climate transitions from breakup of stratocumulus decks under greenhouse warming. *Nature Geoscience*, *12*(3), 163–167. doi: 10.1038/s41561-019-0310-1

Sellers, W. (1969). A global climatic model based on the energy balance of the Earth-Atmosphere system. *Journal of Applied Meteorology*, *8*, 392–400.

Shields, G. A., & Mills, B. J. W. (2017). Tectonic controls on the long-term carbon isotope mass balance. *Proceedings of the National Academy of Sciences*, *114*(17). doi: 10.1073/pnas.1614506114

Siler, N., Roe, G. H., & Armour, K. C. (2018, September). Insights into the Zonal-Mean Response of the Hydrologic Cycle to Global Warming from a Diffusive Energy Balance Model. *Journal of Climate*, *31*(18), 7481–7493. doi: 10.1175/JCLI-D-18-0081.1

Stap, L. B., Berends, C. J., Scherrenberg, M. D. W., van de Wal, R. S. W., & Gasson, E. G. W. (2022, April). Net effect of ice-sheet–atmosphere interactions reduces simulated transient Miocene Antarctic ice-sheet variability. *The Cryosphere*, *16*(4), 1315–1332. doi: 10.5194/tc-16-1315-2022

Stap, L. B., van de Wal, R. S. W., de Boer, B., Bintanja, R., & Lourens, L. J. (2017, September). The influence of ice sheets on temperature during the past 38 million years inferred from a one-dimensional ice sheet–climate model. *Climate of the Past*, *13*(9), 1243–1257. doi: 10.5194/cp-13-1243-2017

Stolper, D. A., Bender, M. L., Dreyfus, G. B., Yan, Y., & Higgins, J. A. (2016, September). A Pleistocene ice core record of atmospheric O2 concentrations. *Science*, *353*(6306), 1427–1430. doi: 10.1126/science.aaf5445

Swanson-Hysell, N. L., & Macdonald, F. A. (2017, June). Tropical weathering of the Taconic orogeny as a driver for Ordovician cooling. *Geology*, G38985.1. doi: 10.1130/G38985.1

Tigchelaar, M., & Timmermann, A. (2016, July). Mechanisms rectifying the annual mean response of tropical Atlantic rainfall to precessional forcing. *Climate Dynamics*, *47*(1-2), 271–293. doi: 10.1007/s00382-015-2835-3

Turbet, M. (2017). CO2 condensation is a serious limit to the deglaciation of Earth-like planets. *Earth and Planetary Science Letters*, 11.

Urey, H. C. (1952). On the early chemical history of the earth and the origin of life. *Proceedings of the National Academy of Sciences*, *38*, 351–363.

Valdes, P. (2011, July). Built for stability. *Nature Geoscience*, *4*(7), 414–416. doi: 10.1038/ngeo1200

Van Der Meer, D. G., Zeebe, R. E., van Hinsbergen, D. J. J., Sluijs, A., Spakman, W., & Torsvik, T. H. (2014, March). Plate tectonic controls on atmospheric CO_2 levels since the Triassic. *Proceedings of the National Academy of Sciences*, *111*(12), 4380–4385. doi: 10.1073/pnas.1315657111

Veizer, J., Godderis, Y., & François, L. M. (2000, December). Evidence for decoupling of atmospheric CO2 and global climate during the Phanerozoic eon. *Nature*, *408*(6813), 698–701. doi: 10.1038/35047044

Velbel, M. A. (1993). Temperature dependence of silicate weathering in nature: How strong a negative feedback on long-term accumulation of atmospheric CO2 and global greenhouse warming? *Geology*, *21*(12), 1059. doi: 10.1130/0091-7613(1993)021⟨1059:TDOSWI⟩2.3.CO;2

Vettoretti, G., Ditlevsen, P., Jochum, M., & Rasmussen, S. O. (2022, April). Atmospheric CO2 control of spontaneous millennial-scale ice age climate oscillations. *Nature Geoscience*, *15*(4), 300–306. doi: 10.1038/s41561-022-00920-7

Volk, T. (1987). Feedbacks between weathering and atmospheric CO2 over the last 100 million years. *American Journal of Science*, *287*, 763–779.

Walker, J. C. G., Hays, P. B., & Kasting, J. F. (1981). A negative feedback mechanism for the long-term stabilization of Earth's surface temperature. *Journal of Geophysical Research*, *86*(C10), 9776. doi: 10.1029/JC086iC10p09776

Westerhold, T., Marwan, N., Drury, A. J., Liebrand, D., Agnini, C., Anagnostou, E., ... Zachos, J. C. (2020, September). An astronomically dated record of Earth's climate and its predictability over the last 66 million years. *Science*, *369*(6509), 1383–1387. doi: 10.1126/science.aba6853

Winnick, M., & Maher, K. (2018). Relationships between CO2, thermodynamic limits on silicate weathering, and the strength of the silicate weathering feedback. *Earth and Planetary Science Letters*, *485*, 111–120. doi: 10.1016/j.epsl.2018.01.005

Zachos, J., Pagani, M., Sloan, L., Thomas, E., & Billups, K. (2001). Trends, rhythms, and aberrations in global climate 65 Ma to present. *Science*, *292*(5517), 686–693. doi: 10.1126/science.1059412

Zeebe, R. E. (2011, July). Where are you heading Earth? *Nature Geoscience*, *4*(7), 416–417. doi: 10.1038/ngeo1196

Zeebe, R. E., & Wolf-Gladrow, D. (2001). *CO2 in Seawater: Equilibrium, Kinetics, Isotopes* (No. 65). Gulf Professional Publishing.

Zhang, L., Hickel, K., & Dawes, W. R. (2004). A rational function approach for estimating mean annual evapotranspiration. *Water Resources Research*, *40*, 1–14. doi: 10.1029/2003WR002710

Zhang, X., Tang, Q., Zhang, X., & Lettenmaier, D. P. (2014, August). Runoff sensitivity to global mean temperature change in the CMIP5 Models: Runoff Sensitivity estimated using CMIP5. *Geophysical Research Letters*, *41*(15), 5492–5498. doi: 10.1002/2014GL060382

Supporting Information for "Deterministic icehouse and greenhouse climates throughout Earth history"

T. Kukla[1], K. V. Lau[2], D. E. Ibarra[3,4], J. K. C. Rugenstein[1]

[1]Department of Geosciences, Colorado State University, Fort Collins, CO

[2]Department of Geosciences and Earth and Environmental Systems Institute, The Pennsylvania State University, University Park, PA

[3]Department of Earth, Environmental and Planetary Sciences, Brown University, Providence, RI

[4]Institute at Brown for Environment and Society, Brown University, Providence, RI, USA

Contents of this file

1. Text S1
2. Figures S1 to S4

Text S1: Sensitivity of the bistability window to climate and geography

The range of global temperatures in which long-term bistability is possible is narrow in our model, restricted to less than $2°C$ in all cases. Two climate parameters appear to determine much of the variability in the long-term bistability temperature range, even across our different geographic configurations: (1) ice albedo and (2) the A term in the climate sensitivity formulation (see main text) (Fig. S3A, B). Higher ice albedo increases the strength of the positive ice albedo feedback that drives bistability, thus also increasing the bistable window. Temperature ranges for bistability only exceed $1°C$ in the highest ice albedo scenarios and in no other simulations. The upper-bound of ice albedo that we simulate here is high compared to average "real world" values due to factors such as melt-ponds, dust, and others that tend to decrease ice albedo. For reference, we include the albedo value assigned to non-melting ice in the Community Atmosphere Model (0.73; magenta line in Fig. S3A).

The temperature response to pCO_2 also influences the range of temperatures where long-term bistability is possible (Fig. S3B). The bistability window is generally smaller when the temperature response to pCO_2 (thus, climate sensitivity) is greater. This result likely emerges from a steepening of the greenhouse temperature-pCO_2 curve, strengthening the feedback and shortening the overall range of bistability (*i.e.* its overlap with the icehouse temperature-pCO_2 curve). While a stronger ice albedo feedback steepens the icehouse temperature-pCO_2 curve climates, it also tends to make the icehouse climate more stable, counteracting this effect and leading to a broader bistability window with a stronger ice albedo feedback. Climate sensitivity does not impact the stability of the greenhouse climate, just the range of overlap it shares with the icehouse state.

For the other parameters there is no clear trend linking the temperature range of long-term bistability with the parameter value. Instead, different geographic configurations show different sensitivities, blurring the overall trend. The water vapor feedback, for example, modifies how sensitive net atmospheric heating is to temperature, similar to climate sensitivity. However, since the temperature profile itself is sensitive to the geographic configuration, the effect of changes in the water vapor feedback term is not uniform across geographies (Fig. S3C).

Different geographic configurations yield different relationships between the range of global temperature and global weathering where long-term bistability is possible (Fig. S4A). In Tropicland world, for example, runoff is highly sensitive to temperature, so the degassing range for long-term bistability increases rapidly with warming (yellow symbols in Fig. S4A). In contrast, the weathering feedback is weaker in Subtropicland world where a broad long-term bistability range for temperature is possible with a narrower degassing range (green symbols in Fig. S4A). The temperature range for short-term climate bistability is positively correlated with, and increases about 3x faster than, that for long-term climate bistability, with no obvious geography-driven trends (Fig. S4B). Thus, the temperature range for long-term bistability remains small even as the short-term bistability range reaches 5-10$°C$.

Figures S1-S4

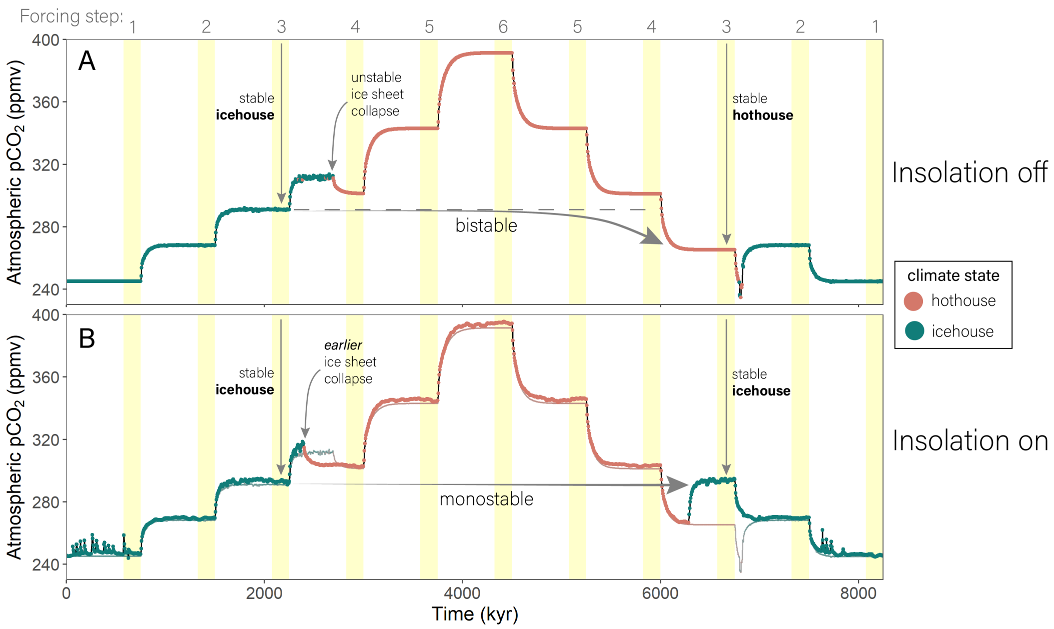

Figure S1. Long-term climate response to volcanism ramp-up/ramp-down. Yellow bars indicate period averaged for figure 3 in the main text. (**A**) Without solar insolation variability forcing step 3 is bistable, with an icehouse occurring if coming from an icehouse, and a hothouse occurring if coming from a hothouse. In forcing step 4 coming from an icehouse, an unstable ice sheet collapses after a few hundred thousand years. Since the glaciated state in step 4 is transient this forcing step is considered monostable. (**B**) With insolation, there is no long-term bistability in step 3 (or any step). Moreover, the ice sheet collapse in step 4 occurs earlier, likely due to reaching an unstable state more quickly due to orbital variability. While long-term climate is monostable, short-term bistability is still evident as lower-pCO_2 hothouse and higher-pCO_2 icehouse states co-exist transiently for forcing steps 3 and 4. The "insolation off" case is reproduced in faded colors of panel B for reference.

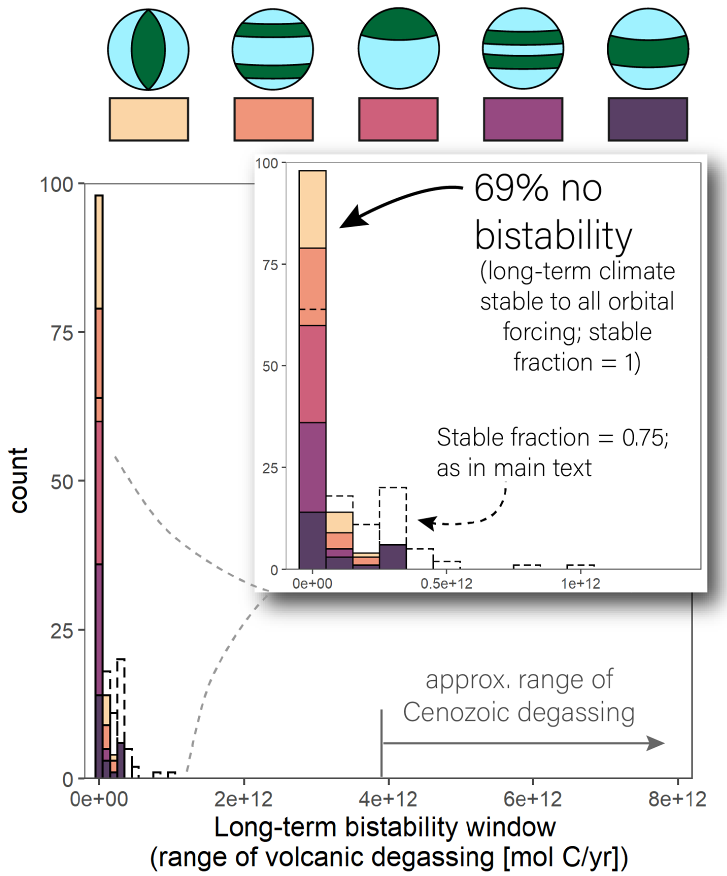

Figure S2. When a given climate state must persist for all orbital forcings to be considered stable in the long-term, the bistability range gets shorter. Dashed lines show the histogram from the main text (with a given climate state persisting for $>$ 75% of orbital configurations). The percentage of solutions with no long-term bistability increases from $\sim$ 50 to nearly 70% as the stable fraction of orbital configurations increases (and, consequently, climate "inertia" decreases).

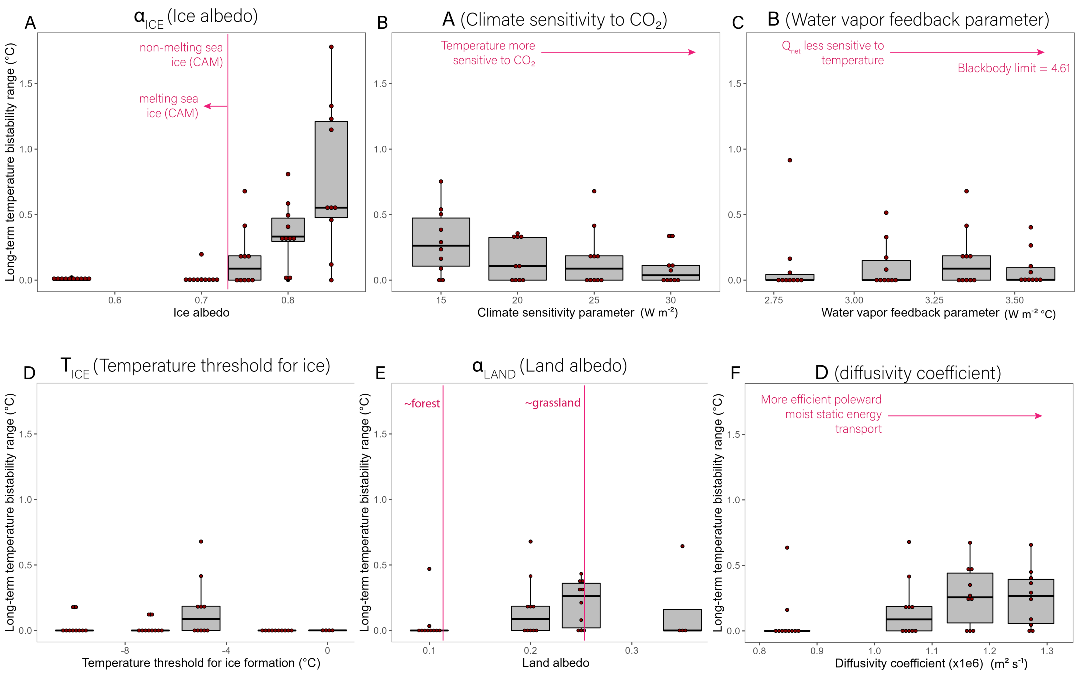

Figure S3. Sensitivity of the global temperature range for long-term bistability to climate parameters. Each box and whisker plot shows simulations across geographies and for a stable fraction of 1 or 0.75 (individual simulations denoted by red dots). (**A**) The long-term bistability range is most responsive to ice albedo, which determines the strength of the ice albedo feedback, although it is most sensitive at high ice albedo values that are likely physically unrealistic. (**B**) The long-term bistability range decreases somewhat with greater cliamte sensitivity. The bistability range for temperature is less sensitive to (**C**) The water vapor feedback term, (**D**) The temperature threshold for ice formation, (**E**) Land albedo, and (**F**) The diffusivity coefficient.

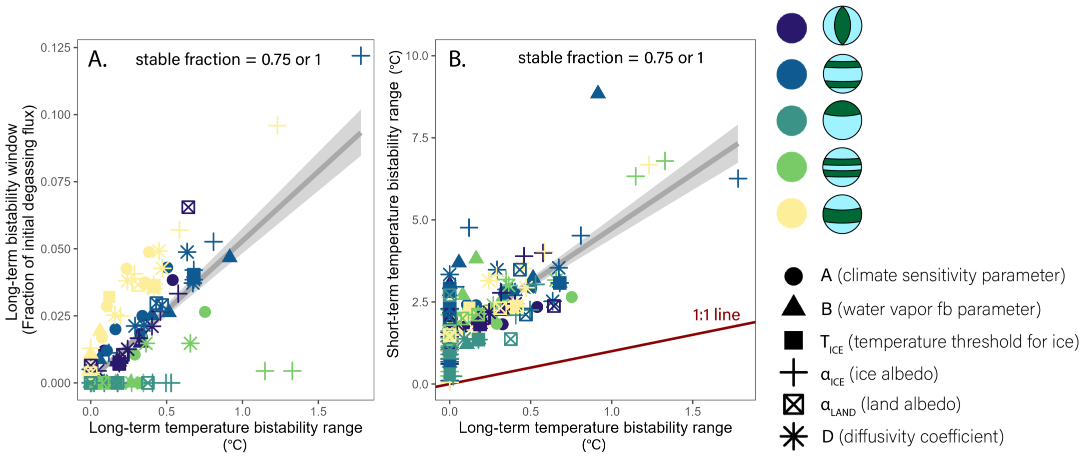

Figure S4. The long-term bistability range for degassing increases with the range for global temperature in simulations where the stable fraction is 0.75 or 1 (**A**). The slope of the increase depends on geography via its control over the weathering response to climate. The temperature range for short-term bistability is correlated with that for long-term bistability (**B**). However, the short-term bistability temperature range increases about 3 times faster than the long-term bistability range.